

Comparative assessment of force, temperature, and wheel wear in sustainable grinding aerospace alloy using biolubricant

Xin CUI^a, Changhe LI (✉)^a, Yanbin ZHANG (✉)^b, Wenfeng DING^c, Qinglong AN^d, Bo LIU^e, Hao Nan LI^f, Zafar SAID^g, Shubham SHARMA^h, Runze LIⁱ, Sujan DEBNATH^j

^a School of Mechanical and Automotive Engineering, Qingdao University of Technology, Qingdao 266520, China

^b State Key Laboratory of Ultra-precision Machining Technology, Department of Industrial and Systems Engineering, The Hong Kong Polytechnic University, Hong Kong, China

^c College of Mechanical and Electrical Engineering, Nanjing University of Aeronautics and Astronautics, Nanjing 210016, China

^d School of Mechanical Engineering, Shanghai Jiao Tong University, Shanghai 200240, China

^e Sichuan Future Aerospace Industry LLC., Shifang 618400, China

^f School of Aerospace, University of Nottingham Ningbo China, Ningbo 315100, China

^g College of Engineering, University of Sharjah, Sharjah 27272, United Arab Emirates

^h Department of Mechanical Engineering, IK Gujral Punjab Technical University, Punjab 144603, India

ⁱ Department of Biomedical Engineering, University of Southern California, Los Angeles, CA 90089, USA

^j Mechanical Engineering Department, Curtin University, Miri 98009, Malaysia

✉ Corresponding author. E-mails: sy_lichanghe@163.com (Changhe LI); zhangyanbin1_qdlg@163.com (Yanbin ZHANG)

© The Author(s) 2022. This article is published with open access at link.springer.com and journal.hep.com.cn

ABSTRACT The substitution of biolubricant for mineral cutting fluids in aerospace material grinding is an inevitable development direction, under the requirements of the worldwide carbon emission strategy. However, serious tool wear and workpiece damage in difficult-to-machine material grinding challenges the availability of using biolubricants via minimum quantity lubrication. The primary cause for this condition is the unknown and complex influencing mechanisms of the biolubricant physicochemical properties on grindability. In this review, a comparative assessment of grindability is performed using titanium alloy, nickel-based alloy, and high-strength steel. Firstly, this work considers the physicochemical properties as the main factors, and the antifriction and heat dissipation behaviours of biolubricant in a high temperature and pressure interface are comprehensively analysed. Secondly, the comparative assessment of force, temperature, wheel wear and workpiece surface for titanium alloy, nickel-based alloy, and high-strength steel confirms that biolubricant is a potential replacement of traditional cutting fluids because of its improved lubrication and cooling performance. High-viscosity biolubricant and nano-enhancers with high thermal conductivity are recommended for titanium alloy to solve the burn puzzle of the workpiece. Biolubricant with high viscosity and high fatty acid saturation characteristics should be used to overcome the bottleneck of wheel wear and nickel-based alloy surface burn. The nano-enhancers with high hardness and spherical characteristics are better choices. Furthermore, a different option is available for high-strength steel grinding, which needs low-viscosity biolubricant to address the debris breaking difficulty and wheel clogging. Finally, the current challenges and potential methods are proposed to promote the application of biolubricant.

KEYWORDS grinding, aerospace, difficult-to-machine material, biolubricant, physicochemical property, grindability

1 Introduction

Mineral cutting fluids have been widely used in the

manufacturing industry for hundreds of years to solve certain technical problems, such as cooling, lubrication and debris removal, under the strong thermal coupling effect of the cutting interface [1–3]. However, traditional processing methods have the following threats:

(i) Non-renewable resource consumption. The annual global consumption of more than 4 million tons of cutting fluids depends on the huge consumption of limited mineral and freshwater resources [4].

(ii) Environmental pollution and workers' health threat. A large amount of oil mist and PM_{2.5} suspended particles are generated by cutting fluids in a high temperature, speed, and pressure processing environment. They are released into the atmosphere, causing irreparable damage to the natural environment and are inhaled by workers, posing a serious health risk [5,6].

(iii) High cost. The cost of cutting fluids is also rising as environmental legislations and environmental inspection policies become more stringent, and treatment may cost up to 18% to 21% of the total cost, which is three to five times the cost of tools (Fig. 1 [7,8]).

Achieving 'carbon neutrality and emission peak' is an important development strategy for China over the next 40 years. Energy saving reform through manufacturing is one of the development focuses of the manufacturing industry. In particular, the transformation and upgrading of the cutting fluid supply mode to green and efficient through technological innovation must be realised [9–11]. Green processing methods based on different ideas, such as, dry cutting [12,13], solid lubrication [14], cryogenic air cooling [15,16], and minimum quantity lubrication (MQL) [17], have been proposed. Biolubricant, as cooling medium in MQL, could reduce the consumption of cutting fluids by more than 90% and has made progress in the application of common materials in cutting [18–20]. Biolubricant is typically produced from vegetable oil or animal fat, and it is biodegradable, non-toxic and eco-friendly [21–23]. Moreover, biolubricant, as an important substitute for traditional mineral oil, can meet the higher demand for sustainable lubricants in the industry and is widely used in various fields [24–26].

Grinding is one of the most important methods of precision forming parts, and the use of grinding fluids exceeds that of cutting fluids [27,28]. In addition, grinding is a crucial process for ensuring manufacturing accuracy and surface quality, especially for aerospace materials, and it accounts for more than 60% of all

processing procedures [29–31]. Accordingly, MQL should be applied in grinding. However, the MQL technology is still constrained by insufficient heat transfer capacity when it comes to aerospace material grinding. These difficult-to-machine materials are more likely to experience thermal damage in the high temperature grinding zone due to their characteristics of low thermal conductivity, high specific grinding energy and fracture toughness [32–34]. The grinding process of titanium alloy [35], superalloy [36,37], high-strength steel [38], composite material [39,40], and other difficult-to-machine materials [41,42] has the serious problems of heavy grinding force, high temperature, and severe wheel wear or clogging [43–45]. The aforementioned issues in MQL grinding must be addressed as soon as possible [46–48]. Nano-enhanced biolubricants, which are prepared by adding nanoparticles in the biolubricant, are expected to improve grindability and meet the demand for green manufacturing [49–51].

Biolubricant, as a vital medium in the manufacturing system, is essential for ensuring machining performance and environmental friendliness [52]. The core problem is to solve heat dissipation, antifriction and antiwear problems through the preparation and use of biolubricant or nano-enhanced biolubricants under extreme grinding conditions. Scholars have carried out a series of experimental studies using vegetable oil as biological cooling medium to evaluate the grinding performance parameters [53–57]. However, the influencing law and knowledge system amongst (1) physicochemical property of lubricants, (2) antifriction and heat transfer behaviour, and (3) machining performance parameters remain unknown. There is no basis for scientific research and industrial application. On this basis, this work conducted a systematic review of biolubricant MQL for machining aerospace difficult-to-machine materials and summarised the influencing mechanism of the physicochemical properties on grindability. The structure of this paper is shown in Fig. 2. Furthermore, the machining performance of titanium alloy, nickel-based alloy, and high-strength steel was reviewed by quantitative evaluation. Finally, this work aims to provide theoretical references for further research by improving the influencing law of biolubricant physicochemical properties on heat dissipation, antifriction, and antiwear.

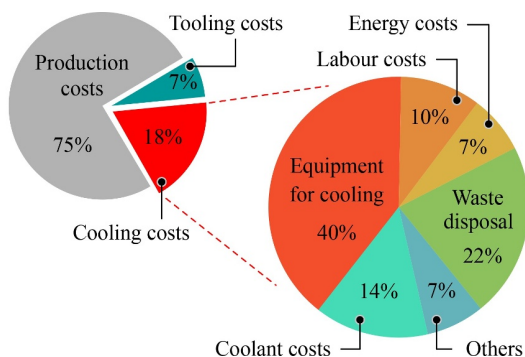


Fig. 1 Distribution of costs in the automobile industry. Reproduced with permission from Refs. [7,8] from Elsevier.

2 Influencing mechanisms of the biolubricant properties on grinding performance

In the early days, mineral oils (e.g., liquid paraffin) were often used as coolant in MQL [58,59]. At present, some studies use mineral synthetic oils (e.g., Castrol limited) [60,61]. Although mineral oil could meet the cooling and lubrication requirement, it is still dependent on

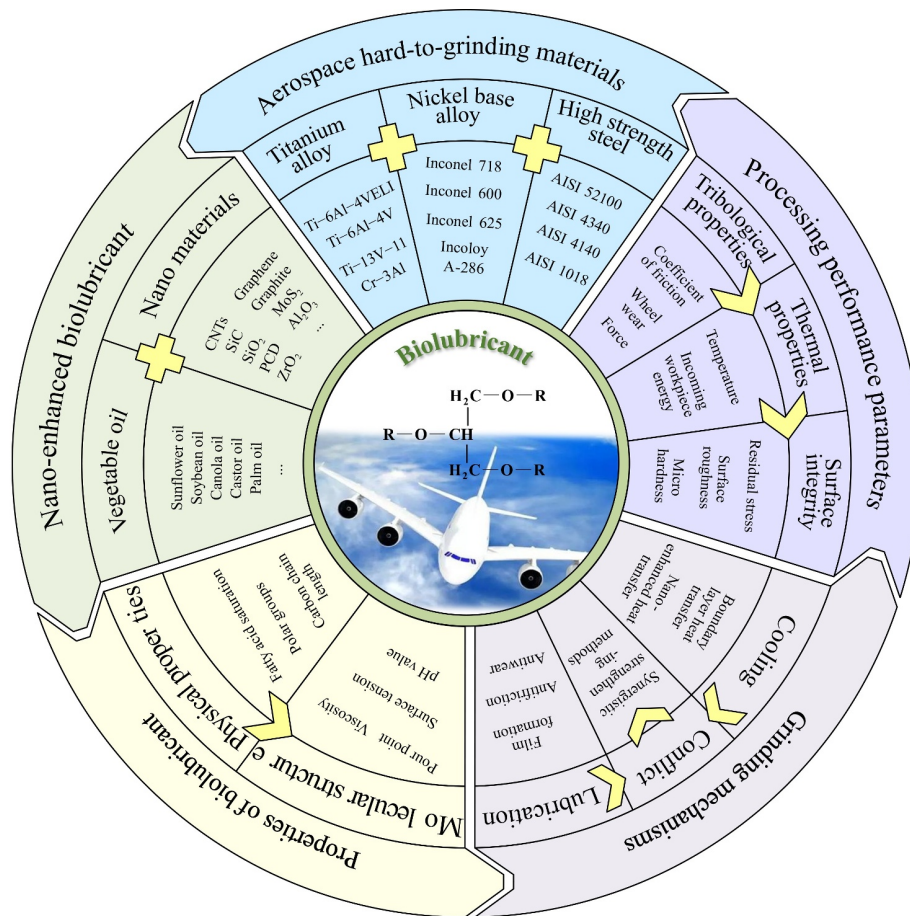


Fig. 2 Paper structure.

non-renewable resources and poses a threat to the environment and workers' health. Kelly and Cotterell [62] used vegetable oil as coolant in MQL drilling experiments for the first time in 2002, and the processing temperature, torque and surface roughness were superior to cutting fluids at a certain drilling speed, launching the exploration into biolubricant application in MQL. Biolubricant is naturally degradable and environmentally friendly, making it perfectly compatible with the original purpose of MQL. The biolubricants currently used for MQL include various vegetable oils (e.g., soybean, palm, peanut, castor, sunflower, rapeseed, sesame, corn, and coconut oil) and synthetic esters (made from degradable components). Zhang et al. [63] and Wang et al. [64] conducted a comprehensive review on the processing properties of vegetable oil lubricants, which involved a confirmatory comparison of the application performance with flood (the usage of cutting fluids) and dry cutting, optimisation analysis of the vegetable oil types considering various machining processes and workpiece materials and revelation of the cooling and lubrication mechanisms.

The main components of vegetable oil are triacylglyceride, a small amount of free fatty acid, part of glyceride, phosphorus ester (0.1%–0.5%), tiny amounts of sterols,

tocopherol and vitamin E [65]. Each triacylglyceride molecule contains three C12–C22 fatty acid chains, including saturated fatty acids (such as palmitic, stearic, and oleic acids) and a variety of unsaturated acids (such as erucic acid, jatropha, and ricinoleic acid). Zhang et al. [63] summarised the molecular types of fatty acids commonly used in vegetable oils at present. Previous research demonstrated that fatty acid carbon chain length, fatty acid saturation (number of C=C double bonds), functional group type, viscosity, surface tension, and pH value are the affecting parameters on cooling and lubrication performance [66]. On this basis, this review comprehensively establishes the influencing law amongst physicochemical property, antifriction and heat transfer behaviour, and machining performance (Fig. 3).

2.1 Grinding performance parameters

The grinding process is a complex interference between abrasive and workpiece. The outermost ring parameters in Fig. 3 are used to evaluate the grindability. Grinding force is the most important indicator, and it consists of material removal force, plough force and interface friction force [67]. The proportion of friction is more than 80% due to the negative rake cutting characteristics of the

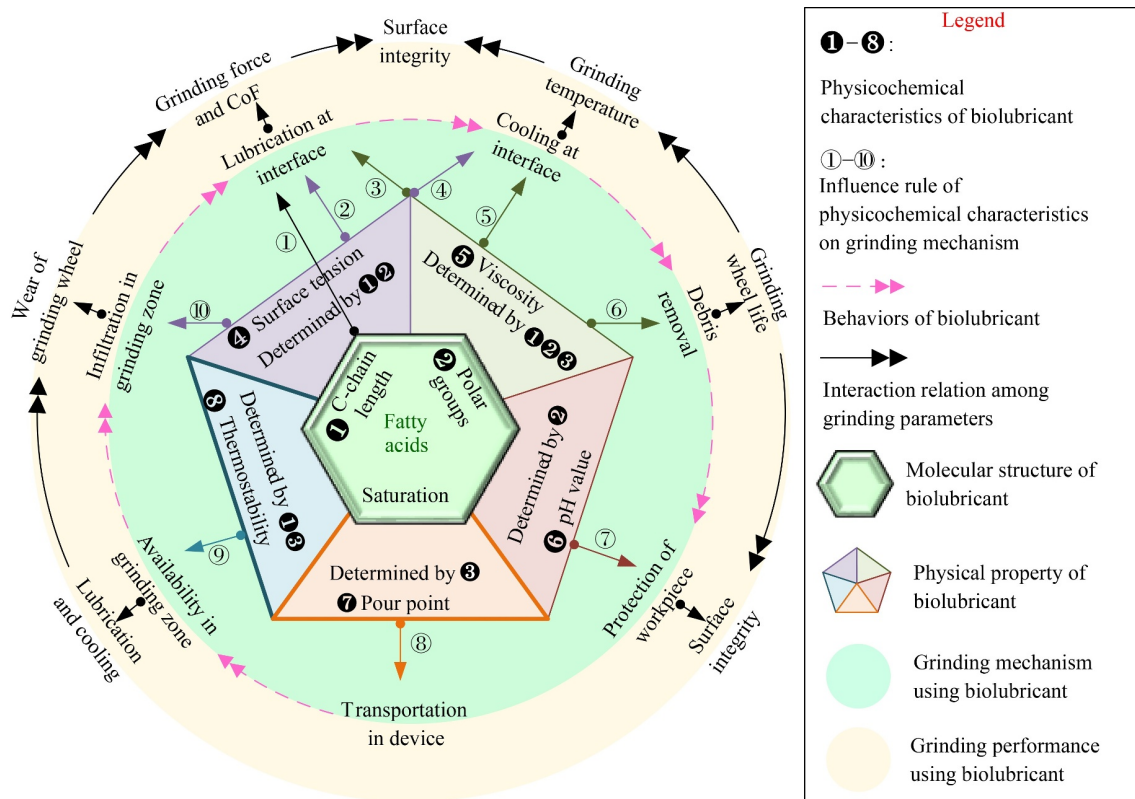


Fig. 3 Grinding mechanisms using a biolubricant. CoF: coefficient of friction.

abrasive. Therefore, the reduction of grinding force under different lubrication conditions is mainly the reduction of friction. Furthermore, coefficient of friction (CoF) is used to evaluate lubrication performance.

The grinding force value is the main parameter used to analyse not only the tribological characteristics of the interface but also the grinding heat output and dissipation. The total heat flux density (Q_{total}) generated per unit time in the grinding zone is related to the grinding force [68,69]. The four transfer outlets of grinding heat, are the heat flux density of a workpiece (q_w), the heat flux density of abrasive (q_a), the heat flux density of debris (q_d), and the heat flux density of the cooling medium (q_c). Increasing q_c is one of the feasible methods for reducing the maximum surface temperature of a workpiece. Thus, cooling performance is also a key property influencing grinding temperature.

The material removal strain rate is much higher than that of cutting due to the negative rake cutting in the process of abrasive removal [70,71]. The debris is C-shaped, and the free surface is shear band shape. The tribological and heat transfer characteristics of the rake face/debris interface during material removal can be analysed by the degree of finishing of the debris side and the fresh surface and the regularity of the shear band on the free surface.

The grinding wheel wear and life are dependent on lubrication infiltration and debris removal ability of the

cooling conditions. The forms of wheel wear include abrasive loss, adhesion blockage, and abrasive shedding. In addition, the material volume removed per unit volume of wheel wear (G-ratio) is also one of the parameters that reflect the life of wheel, and the larger the G-ratio is, the smaller the degree of wheel wear is and the longer the service life will be [72].

Surface integrity is comprehensively influenced by the above-mentioned parameters. Surface roughness, surface burn, adhesion, and other phenomena are key indicators for surface integrity evaluation. The surface roughness (Ra) of the workpiece reflects the average height of the micro-convex peak and micro-concave valley on the workpiece surface [73]. Thermal boundary removal and material constitutive changes occur due to the shift in lubrication conditions, which have a significant effect on surface roughness [74,75].

2.2 Molecular structure of fatty acids

The molecular structure of biolubricants is composed of one glyceride and three straight-chain fatty acids. The carbon chain length of a fatty acid molecule ranges from 14 to 22, including saturated and unsaturated fatty acids. Different fatty acids and their contents in biolubricants determine their physicochemical properties, which affects the cooling and lubrication performance in grinding (**Mechanism ①**).

The polar atoms (S, O, N, etc.) and polar groups (–OH, –COOH, –COOR, –COR, –CN, etc.) contained in lubricant have excellent affinity. Physical adsorption occurs with metal material molecules through van der Waals force [76], forming a physical adsorption film with antifriction and antiwear, thus reducing the grinding force. However, fatty acids and triglycerides in biolubricants contain polar groups, thus forming a lubricating oil film with high strength, which improves the lubrication performance of the grinding zone. In addition, fatty acid compounds undergo metal saponification reaction on the metal surface during a high-temperature grinding process, forming a semi-chemical bonded oily film with a single molecular layer with vertical adsorption characteristics. The compact adsorption on the workpiece material surface under intermolecular force increases tool life [77]. Regardless of physical adsorption or chemical reaction, the factors affecting the strength of lubricating film are fatty acid saturation and carbon chain length.

The strength of the physical adsorption film formed by biolubricants containing saturated fatty acids is higher than that formed by unsaturated fatty acids, and the less C=C double bonds in unsaturated fatty acids, the higher the strength of the lubrication film. This phenomenon is due to the easy oxidation of the polar C=C double bond leading to the degradation of biolubricants, reducing their thermal stability and oxidation resistance and resulting in the failure of the physical adsorption film. In addition, fatty acids without C=C double bond and linear molecular chain can form a tighter fatty acid molecular structure with a compact and uniform shape, which improves the strength and lubrication performance of film.

When the number of C atoms in saturated fatty acids is greater than 16, the increase in C atom number will not affect its frictional properties. In unsaturated fatty acids, the density of the adsorbed film is reduced due to the adsorption effect of the oleic bond on the polar unsaturated bond, thus reducing the strength and lubrication performance of the oil film. Accordingly, the number of C atoms in the saturated and unsaturated fatty acids is the same, and the lubrication film performance of the unsaturated fatty acids is poor. Meanwhile, the cohesion between molecules is proportional to the number of C atoms. Thus, the strength and lubrication performance of the adsorption film of the unsaturated fatty acids with long carbon chain length are stronger than those with short carbon chain length.

2.3 Viscosity of biolubricant

Viscosity is the variable exchange and adhesion generated by regular intermolecular motion and is one of the main factors that affect the cooling and lubrication performance of biolubricants [78]. The viscosity of lubricant mainly affects its wetting, lubrication and heat transfer performance in grinding.

(i) Influence of viscosity on debris removal (**Mechanism ⑥**). After the lubricant enters the grinding zone at a certain speed and angle, the fluidity of the lubricant with high viscosity becomes poor due to the viscous force, and it cannot fully penetrate into the wheel–workpiece interface and take away the debris.

(ii) Influence of viscosity on cooling performance (**Mechanism ⑤**). The lubricant entering the grinding zone flows at a certain speed, and the relative motion of the liquid layer is also carried out during the relative motion of the lubricating oil film formed on the wheel–workpiece interface. Accordingly, the heat transfer process of the lubricant microdroplet conforms to the convective heat transfer theory of flowing liquid, and the heat transfer coefficient is related to viscosity. When the Reynolds number of the lubricant is much larger than 2300, the oil film in the grinding zone carries out convection heat transfer in the way of turbulence. According to the heat transfer theory, the temperature gradient of the thermal boundary layer is the largest in the viscous bottom layer and gently changes in the turbulent branch layer. Consequently, the heat transfer performance of lubricant is determined by the viscous bottom layer. Thus, the greater the viscosity of lubricant, the thicker the viscous bottom layer, the smaller the temperature rise per unit time and the lower the heat transfer capacity.

(iii) Influence of viscosity on lubrication performance (**Mechanism ③**). Reducing the interfacial friction between the abrasive rake face/debris and the back face/fresh surface of the workpiece can reduce the heat generated by the friction, lower the temperature and improve the lubrication performance. After the lubricant enters the grinding zone, the lubricant with higher viscosity has better lubrication performance because of the difference in wettability.

2.4 Surface tension of biolubricant

When lubricant microdroplets enter the grinding zone, the smaller the surface tension is, the smaller the particle size and the more uniform the distribution of the droplets will be. Moreover, the contact angle of the droplet is small; thus, it has a larger infiltration area per unit particle size volume. In conclusion, the wettability and lubrication of biolubricant was improved (**Mechanism ②**).

Meanwhile, surface tension further affects the cooling performance through the influence of contact angle. This concept is mainly reflected in two aspects:

(i) The smaller the surface tension is, the smaller the contact angle of the microdroplet is, which increases the wetting area and further provides the cooling performance of lubricant (**Mechanism ⑩**).

(ii) The residence time of lubricant microdroplets is considerably short after entering the grinding zone, and they are rapidly carried out of the grinding zone with the wheel. According to the principle of convective heat transfer, the two parts in convective heat transfer are as

follows: thermal boundary layer and mainstream region. The thickness of the thermal boundary layer is basically unchanged. However, the lubricant in the mainstream region is not fully absorbed enough heat away in the particularly short cooling time and does not play a good heat transfer role. When the contact angle of the microdroplet is reduced, the thermal boundary layer area increases, and the proportion of grinding fluids in the mainstream region decreases, improving the cooling performance (**Mechanism ④**).

2.5 pH value of biolubricant

The influence of acid-base property, as a lubricating medium in cutting, on the surface quality of parts is reflected after they are processed [79]. Alkaline lubricants tend to passivate metal surfaces or form insoluble hydroxide or oxide film layers. The acid lubricant will promote the single displacement reaction to corrosion of metal, but it will also make the synthetic esters have incomplete hydrolysis reaction, affecting the processing effect. Biolubricants are typically acidic, especially during the preparation of synthetic ester biolubricants, to increase the antiwear performance. A variety of polar functional groups ($-\text{OH}$, COOH , $\text{R}-\text{O}-\text{R}'$, etc.) are added to the carbon chain. The carboxy group ionises hydrogen ions in an aqueous solution, making the lubricant acidic. Therefore, the preparation of synthetic esters requires the addition of some amines (amine is alkaline in the aqueous solution, and the representative substance is diethylene glycol amine) for neutralisation to alkaline (**Mechanism ⑦**).

2.6 Pour point of biolubricant

The proper pour point of biolubricant is the premise of its effectiveness. Pour point is the lowest flow temperature of biolubricant, which is a conventional index for characterising the low temperature fluidity. The pour point of vegetable oil is between -15 and -19 °C, which is higher than that of mineral oil, because of the large amount of $\text{C}=\text{C}$ double bond in vegetable oil. Biolubricants stored in microlubricant supply units will lose their fluidity and cannot be properly transported if the ambient temperature is considerably low. The influence of vegetable oil pour point should be considered. For example, in northeast China, Russia, and other countries and regions, vegetable oil cannot be used when the ambient temperature is lower than 20 °C. Therefore, the reduction of pour point has become one of the research topics of biolubricants (**Mechanism ⑧**).

Tao and Li [80], from Shanghai University, disclosed a technology that improved the oxidation resistance and pour point of vegetable oil by saturated isomerisation of double bonds. They used the epoxidation process to saturate $\text{C}=\text{C}$ double bonds, etherification reaction to

obtain fatty alcohol ether and esterification reaction to acquire synthetic oil esters. The pour point of castor oil was reduced from -35 to -58 °C by technology, and that of rapeseed oil was reduced from -18 to -29 °C. Zhang et al. [81] from Beijing University of Chemical Technology published a method for preparing low pour point biolubricant from green modified plant-based derived oil, which reduced the pour point of biolubricant, which contained oleic acid as the main component, to -70 °C and increased the flash point to 298 °C. Scholars proposed a ‘two-step method for preparing polyol ester lubricating oil’, with the pour point reduced to -50 °C and flash point increased to 305 °C.

2.7 Thermostability of biolubricant

The thermal stability of biolubricants at high temperature boundary in the grinding zone is the premise of effective cooling and lubrication, and flash point is an important parameter in characterising its thermal stability. The flash point of vegetable oil is generally about 280 °C, with soybean and cottonseed oil being 280 °C, rapeseed oil being 275 °C, and peanut oil being 285 °C. When the flash point is lower than the grinding temperature, the vegetable oil will fail. In addition, the density of $\beta\text{-H}$ and electron cloud on the carbon framework of vegetable oil is large, and it is easy to be decomposed by heat at high temperature. $\text{C}=\text{C}$ double bonds can be found in branched fatty acids, and they can easily decompose at a high temperature. In vegetable oil modification, epoxidation + ring-opening reaction, selective hydrogenation and hydrogenation cracking are commonly used for $\text{C}=\text{C}$ double bonds. Polyols without $\beta\text{-H}$ can be esterified or transesterified with fatty acid or fatty acid ester to prepare polyol ester lubricating base oil (**Mechanism ⑨**).

Wang and Shen [82], from Shanghai Zhongfu Special Oil Co., Ltd., disclosed a patent named as ‘an environmentally friendly vegetable oil transformer oil and its preparation method’, which improved the flash point to 350 °C by ‘hydrogenation and two alkaline washing’ modification of rapeseed oil and peanut oil. However, the improvement of thermal stability of vegetable oil is still a difficult problem to be solved for grinding applications.

3 Grindability of aerospace alloy using biolubricant

Scholars have initially carried out the exploration of biolubricant as a lubrication medium in grinding for typical aerospace difficult-to-machine materials, such as titanium alloy, nickel-based alloy, and high-strength steel [83,84]. The research is mainly divided into four stages: validation experimental study, comparative study of biolubricants, exploration of nano-enhanced biolubricants, and adaptation of nanomaterials to biolubricants.

3.1 Titanium alloy

The types of titanium alloys mainly include Ti-6Al-4V (TC4), Ti-6Al-4VELI and Ti-13V-11Cr-3Al, which are used to engine blades, compressor discs, landing gear, heat shields, etc. The chemical composition and mechanical properties of the commonly used Ti-6Al-4V are shown in Tables 1 and 2. The grinding problems of titanium alloys come from three aspects: enhanced mechanical activity, extremely low thermal conductivity, and low elastic modulus [85,86]. Therefore, this research

Table 1 Chemical composition of Ti-6Al-4V

Chemical composition	Mass ratio/wt.%
Al	6.180
V	4.190
Fe	0.300
O	0.150
N	0.050
C	0.100
H	0.015
Ti	Balance
Si	0.150

focuses on the workpiece surface integrity and grinding force/heat performance parameters [87,88].

3.1.1 Force and CoF

Many experimental studies have been carried out on the grinding force of titanium alloy. Sadeghi et al. [89] observed a large normal and tangential force reduction of 72.2% and 61.9%, respectively, compared with soluble oil when using biolubricant in MQL for Ti-6Al-4V, as shown in Fig. 4 [89-91]. However, the normal and tangential forces in the synthetic ester MQL were reduced by 16.7% and 20.5% compared with biolubricant MQL, respectively. This notion confirms the feasibility of replacing water-soluble cutting fluids with biolubricants. The grinding force can be significantly improved because of the excellent lubrication performance of biolubricants, which produce low friction and better debris removal performance. Meanwhile, synthetic esters with certain chemical modifications have better grinding performance than biolubricants. The reason is that synthetic esters have good lubricity and film strength and high temperature resistance, which can more effectively reduce friction than biolubricants. Li et al. [90] used biolubricant MQL in TC4 grinding and found that the normal and

Table 2 Mechanical properties of Ti-6Al-4V

Material	Hardness	Yield strength	Elongation	Tensile strength	Elasticity modulus	Density	Thermal conductivity	Specific heat
Ti-6Al-4V	30 HRC	861 MPa	14%	993 MPa	114 GPa	4.43 g/cm ³	5.44 W/(m·K)	526.3 J/(kg·K)

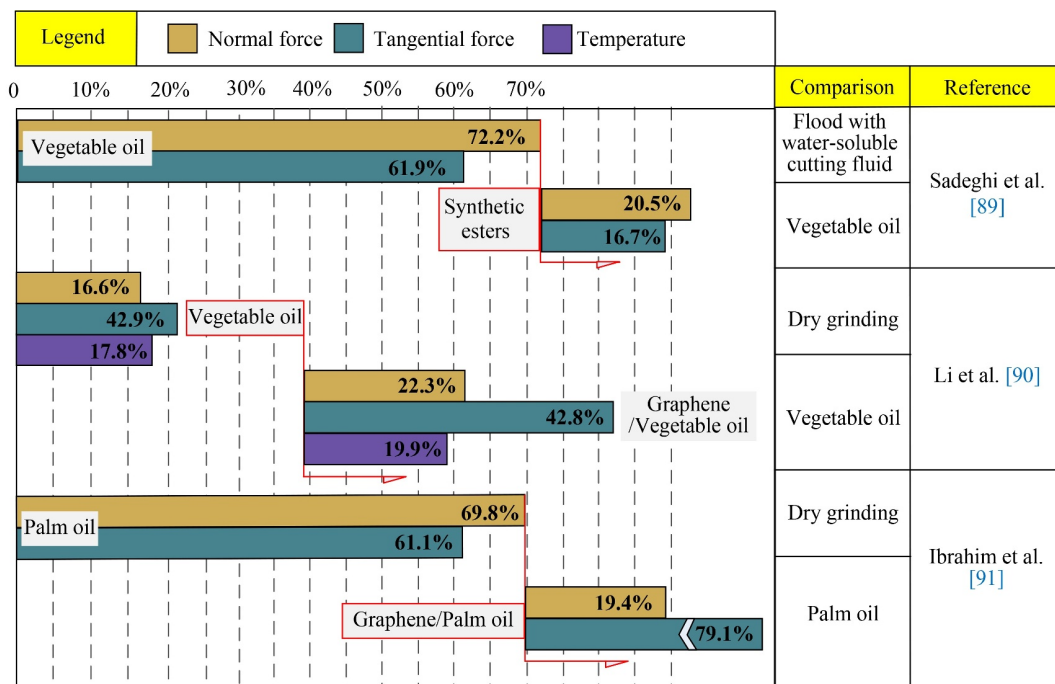


Fig. 4 Improvement ratio of biolubricant MQL compared with the traditional flood or dry grinding [89-91].

tangential forces decreased by 16.6% and 42.9% compared with dry grinding, respectively. Furthermore, the advantage of biolubricant could be reflected by the CoF, which decreased from 0.562 to 0.384. Ibrahim et al. [91] also obtained a lower CoF compared with flood and dry grinding when using palm oil and synthetic esters as a lubrication medium. Based on the above-mentioned verification results, biolubricants and vegetable synthetic esters are more conducive to the formation of lubricating oil film compared with mineral fluids due to their unique molecular structure (long molecular chain, polar group), thus obtaining better interface tribological properties.

Research on the grinding performance of the different biolubricants is the premise of process optimisation. Singh et al. [92] compared the grindability using canola, soybean and olive oil as lubricating media in Ti-6Al-4VELI grinding. Amongst the three oils, canola oil obtained the lowest grinding force (tangential grinding force $F_t = 4.68$ N, normal grinding force $F_n = 15.25$ N), CoF (0.307) and specific grinding energy (17.16 J/mm³). The viscosity of canola oil reaches 38 mPa·s at 40 °C, whilst those of the soybean and olive oil are 26 and 32 mPa·s, respectively. This finding indicated that viscosity plays a key role in improving the tribological characteristics.

In terms of molecular structure, the main fatty acid composition of canola oil is erucic acid (C22:1), which has higher straightness and longer carbon chain.

Meanwhile, the main fatty acid compositions of soybean and olive oil are linoleic acid (C18:2), with lower straightness and shorter carbon chain, and oleic acid (C18:1), with higher straightness and shorter carbon chain. Thus, canola oil achieved the best lubrication performance.

When graphene was introduced to prepare nano-enhanced biolubricants by Li et al. [90], the normal and tangential grinding forces were 22.3% and 42.8% lower than those of the biolubricants due to their excellent antifriction and enhanced heat transfer characteristics, and the CoF was also reduced to 0.283. Ibrahim et al. [91] also found a significant improvement in lubrication when graphene was added. The tangential grinding force was reduced by 79.1%, and the normal grinding force was lowered by 19.4% compared with those of pure palm oil. Moreover, the CoF was reduced from 0.247 to 0.061.

A lubricating oil film was found on the workpiece surface by energy dispersive spectrometry (EDS) analysis at three different points, as shown in Fig. 5 [91]. The carbon element content at A, B, and C positions are 18.22%, 34.43%, and 19.79%, respectively, whilst the carbon content in the Ti-6Al-4V sample is less than 0.03%. Therefore, the presence of a large amount of carbon content is attributed to the formation of graphene lubrication films during the lubrication of a graphene nano-enhancer with biolubricants. Setti et al. [93] reported that the use of an Al₂O₃ nano-enhanced biolubricant

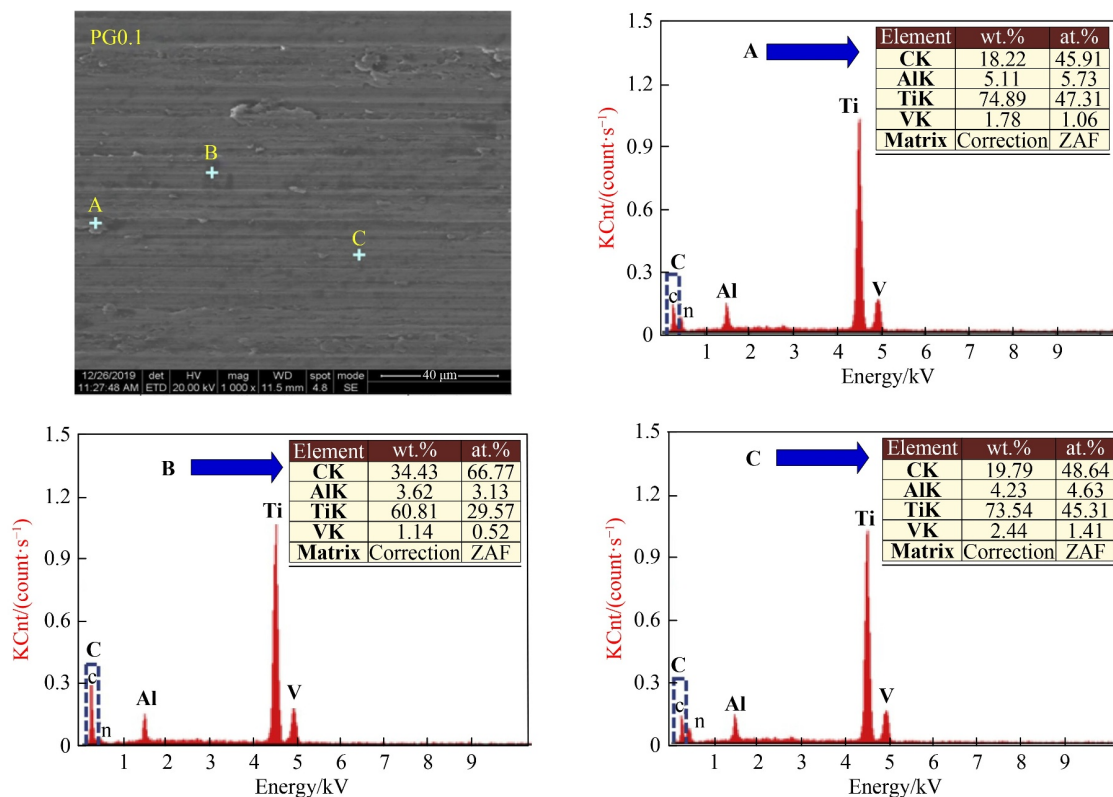


Fig. 5 Lubricant film observation by EDS analysis. Reproduced with permission from Ref. [91] from Elsevier.

significantly reduced the CoF as the grinding time increased, whilst dry grinding and flood did not have this gain effect. This advantage was explained by the discovery of a lubricating oil film on the workpiece surface, and EDS analysis fully confirmed the contribution of the nano-enhancers.

The suitability of nano-enhancers and biolubricants has a significant effect on the grinding performance of the nano-enhanced biolubricants, which is mainly reflected in different types and mass fractions of the nano-enhancers. Singh et al. [92] used layered nano-enhancer graphene, graphite and MoS₂ to prepare nano-enhanced biolubricants with sunflower oil. The results showed that graphene achieved the lowest CoF (0.253) and specific grinding energy (12.76 J/mm³). When the mass fraction of graphene is increased, the grinding performance parameters increase first and then decrease, and the optimal mass fraction of graphene and canola oil was 1.5 wt.%. The increase in concentration improved the number of nano-enhancer for effective lubrication at the interface and increased the viscosity of the biolubricant [94]. However, the nano-enhancer will aggregate, precipitate and fail when the concentration is considerably high. How to prevent agglomeration and improve the optimal mass fraction is also a current research focus.

3.1.2 Wheel wear

Cubic boron nitride (CBN) and silicon carbide wheels are used in titanium alloy grinding, and the lubrication performance of biolubricant has a significant effect on wheel wear and life [95]. Ibrahim et al. [91] carried out a friction and wear experiment using zirconia balls and titanium alloy workpiece to simulate the grinding

conditions. Experimental results showed that wear rate with synthetic ester (LB2000) and palm oil are significantly reduced compared with dry lubrication. In comparison with palm oil, the wear rate decreased by an order of magnitude to 3.65×10^{-4} when graphene was selected as a nano-enhancer. Setti et al. [93] observed the wheel wear under different lubrication conditions, as shown in Fig. 6 [93]. An obvious wear plane was formed on the abrasive surface under poor lubrication performance in dry grinding. When nano-enhancers were used, the wear phenomenon was significantly controlled, and good abrasive sharpness was maintained. Under high-pressure impact, the nano-enhancers enter the pore of wheel for cooling and lubrication. Meanwhile, the sliding/rolling of nano-enhancers prevents the direct contact between the wheel and the workpiece. In addition, nano-enhancers promote the discharge of debris from the pore of the wheel and keep the wheel clean with the effect of MQL pressure. Liu et al. [96] indirectly characterised the sharpness and wear of grinding wheel by observing the material removal rate (Λ_w). The result showed that the material removal rate of the synthetic ester-based nano-enhancer was 71.8% higher than that of flood. Thus, the excellent lubrication performance of the nano-enhancer biolubricant is verified.

3.1.3 Grinding temperature

The burn of the workpiece surface in titanium alloy grinding is intriguing because the frictional heat gathers on the workpiece surface [97]. The grinding temperature in vegetable oil MQL obtained by Li et al. [90] is 229.18 °C, which is 17.8% lower than that of dry grinding, as shown in Fig. 4. After a graphene nano-

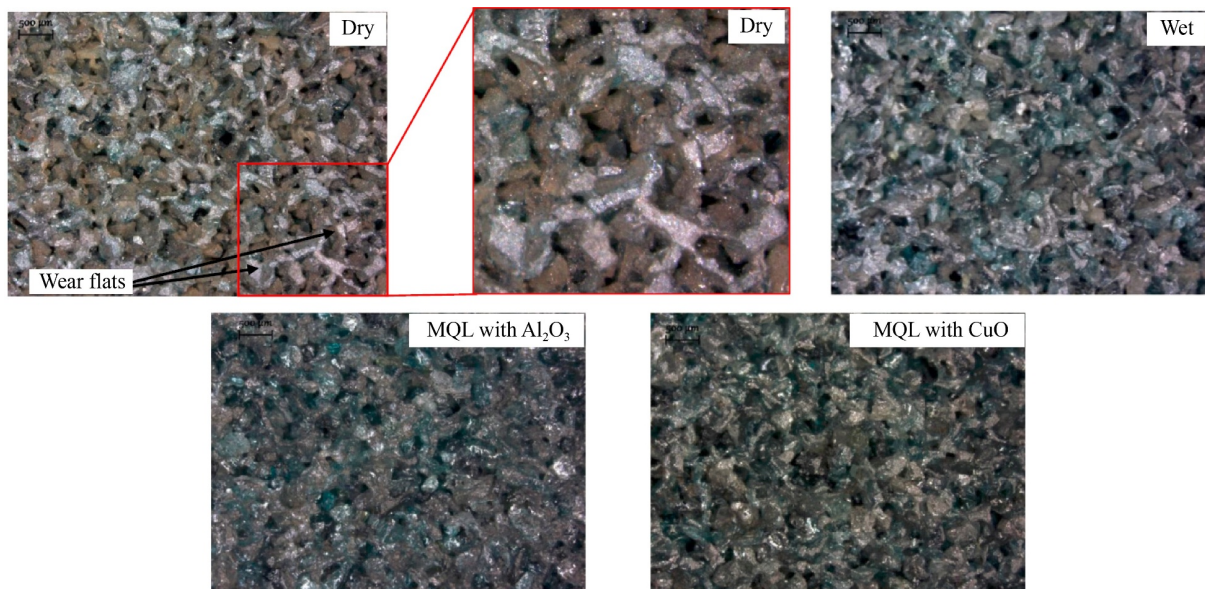


Fig. 6 Grinding wheel wear under different lubrication conditions. Reproduced with permission from Ref. [93] from Elsevier.

enhancer was added, the temperature decreased to 183.61 °C, which is 34.2% lower than that of dry grinding. Liu et al. [96] carried out a multi-factor experimental study of Ti-6Al-4V grinding, amongst which cooling condition (four levels: dry grinding, flood, MQL, and nanolubricant minimum quantity lubrication (NMQL)) was one of the factors. NMQL can obtain a higher S/N value compared with dry and MQL grinding, indicating that nano-enhanced biolubricants are most effective in reducing grinding temperature. Furthermore, the lowest temperature reached 133.8 °C in NMQL.

The addition of nano-enhancers changes the biolubricants from pure oil to two-phase fluid, resulting in the formation of microclusters with nano-enhancer as the core and oil as the coating layer. The Brownian movement effect of the microclusters will significantly improve the heat transfer performance [98]. In addition, the viscosity and surface tension of the biolubricants will change in a beneficial direction. The reduction of grinding temperature depends on the improvement of the heat transfer performance of the lubricating medium, which conforms to the convection heat transfer mechanism [99,100]. Convective heat transfer coefficient is a key factor that affects convective heat transfer capacity. Yang et al. [101] established a convective heat transfer coefficient formula under NMQL. According to the formula, the main factors affecting convective heat transfer coefficient include specific heat capacity, viscosity and thermal conductivity of biological lubricants, thermal

conductivity, specific heat capacity, content of nanomaterials and Brownian movement activity of nano-enhancers, and so on. The above-mentioned factors can be used as the basis for heat exchange performance optimisation of NMQL.

3.1.4 Debris morphology

Cui et al. [102] observed the debris morphology in the grinding experiment of Ti-6Al-4V under different lubrication conditions, as shown in Fig. 7 [102], including dry grinding with cryogenic air (−5 °C) and NMQL with Al₂O₃/synthetic ester nano-enhanced biolubricant. In dry grinding, no lubricant can be found in the abrasive/debris interface, resulting in obvious furrow marks on the fresh surface of debris (due to the fast abrasive wear). In addition, the fresh surface of the debris is accompanied by material adhesion and accumulation, which is the material flow accumulation caused by the increase in plasticity and interfacial friction of debris under high temperature. Furthermore, the side of debris is rough and has a zigzag defect formed after the material pulling fracture, which is caused by the material's strong local plasticity at high temperature. Finally, the distribution of free surface shear bands is chaotic. This phenomenon is due to the poor tribological properties of the interface that results in the stuttering and crawling phenomena during the material removal. The above-mentioned phenomenon has been significantly improved in NMQL. However, in

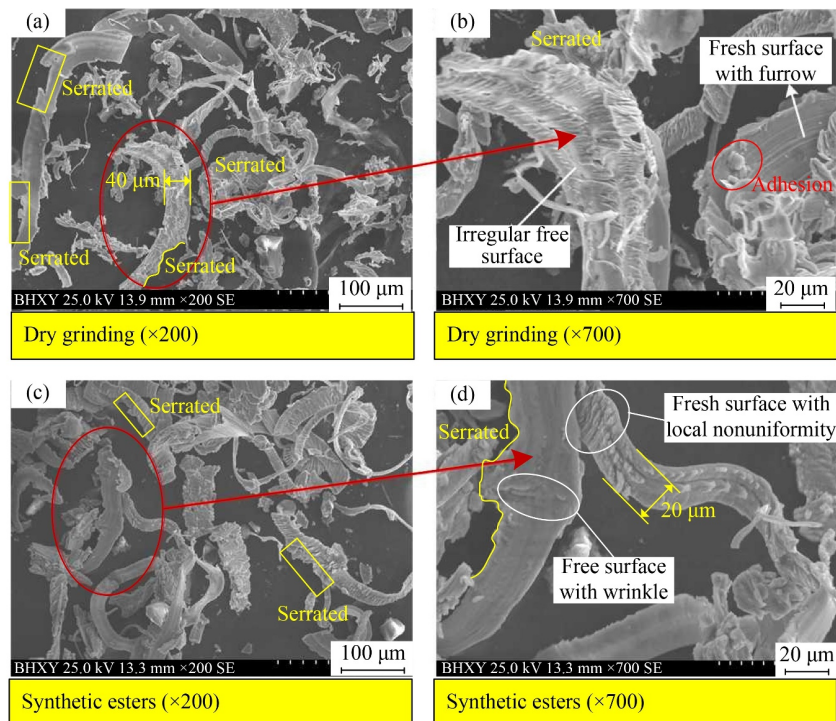


Fig. 7 Debris morphology under different lubrication conditions: (a) dry grinding (×200), (b) dry grinding (×700), (c) synthetic esters (×200), and (d) synthetic esters (×700). Reproduced with permission from Ref. [102] from Elsevier.

some cases, the fresh surface is still rough, the side has a serrated defect, and the free surface is not uniform. The thermal softening effect in the material removal process results in plastic enhancement and fracture stress reduction due to the high mechanical and thermal loads. This phenomenon increases the critical cutting depth, debris width, plastic accumulation on both sides of the furrow and material adhesion between the workpiece and debris surface [103]. Setti et al. [93] found that the debris length is larger in dry grinding and flood compared with NMQL.

3.1.5 Surface integrity

In the study of Sadeghi et al. [89], the surface roughness was reduced to 0.2–0.31 μm by using vegetable oil and synthetic esters as lubricating media. The surface roughness of the synthetic ester is lower than that of vegetable oil under different flow rates. Li et al. [90] found that the R_a value of vegetable oil MQL could be reduced to 0.438 μm , which is 28.40% lower than that with dry grinding. Furthermore, the R_a value was reduced to 0.295 μm , which was 51.80% lower than that of dry grinding, when graphene nano-enhanced biolubricant was used. When palm oil was used, the R_a value reached 0.325 μm , which was 43.97% lower than that of flood. When graphene is mixed with palm oil, the R_a value reached 0.278 μm , which was 52.07% lower than that of flood [91]. However, the surface roughness ranges from 0.6 to 0.7 μm , which is at the same level as that of dry grinding, when water-based nanofluids were used [93]. Biolubricants have been confirmed to have a significant effect on improving surface roughness. According to the comparison of the different vegetable oils, the surface

roughness of canola, soybean, olive and sunflower oil fluctuated in the range of 0.41–0.44 μm , and canola oil had a slight advantage. The R_a value significantly increased after a nano-enhancer was introduced, and the lowest value was 0.210 μm . When the nano-enhancer concentration changes, R_a value and grinding force change in the same rule, and an optimal mass fraction exists.

The microhardness of the workpiece surface reflects the material property change under the influence of machining heat/force. In the study of Li et al. [90], the microhardness value reached 431.53 HV in dry grinding, whilst it decreased to 391.69 and 349.37 HV when vegetable oil and nano-enhanced biolubricant were used, which were 9.2% and 19.0% lower than those of dry grinding. The decrease of force and temperature results in the decrease of the thermally affected layer thickness on the workpiece surface and microhardness.

The surface morphology of the workpiece can directly reflect the machining defects. The suppression of surface defects formed by machining is the most important method to improve the surface integrity. The common surface defects in titanium alloy grinding include adhesion, burn, plastic accumulation and scratch. According to Sadeghi et al. [89] (Fig. 8), plastic deformation, thermal damage (such as debris adhesion and surface deposition) significantly reduced in vegetable oil and synthetic ester MQL condition compared with flood. When Li et al. [90] used a biolubricant, grinding burns were avoided. However, adhesion and wide furrows still existed. Meanwhile, the optimal workpiece surface was obtained without obvious defects when 0.1 wt.% concentration of graphene nano-enhanced biolubricant was used. Ibrahim et al. [91] also obtained the same conclusion. Singh et al. [92] found that plastic uplift existed in flood, and large

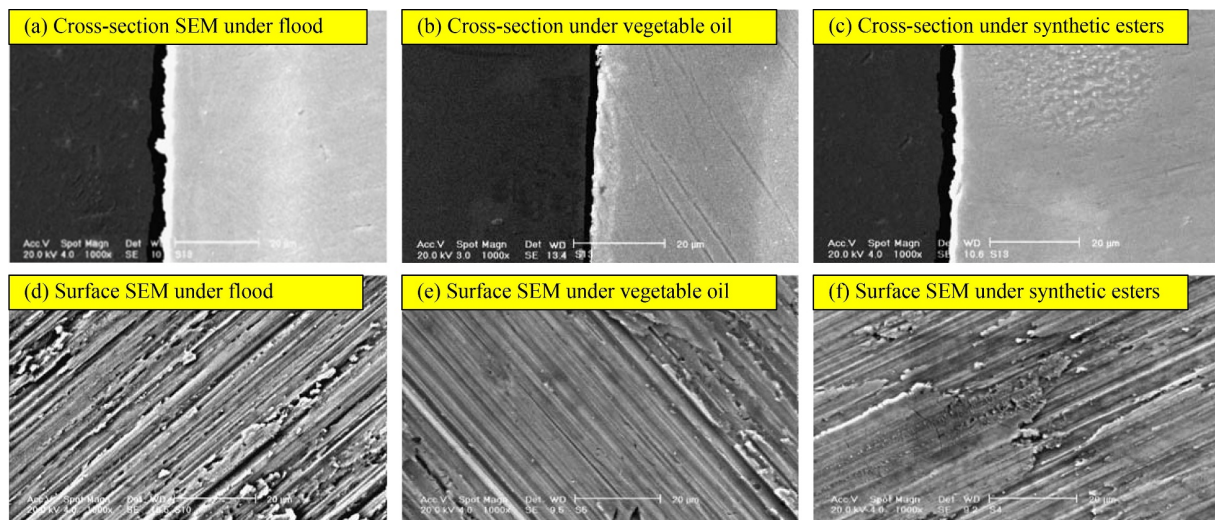


Fig. 8 Surface and cross-section morphology under different lubrication conditions: cross-section scanning electron microscopy (SEM) under (a) flood, (b) vegetable oil, and (c) synthetic esters; surface SEM under (d) flood, (e) vegetable oil, and (f) synthetic esters. Reproduced with permission from Ref. [89] from Springer Nature.

grinding burns occurred in dry grinding. The workpiece surface under canola oil MQL was still rough even though the plastic uplift defects were reduced. Graphene/canola oil NMQL achieved a smoother workpiece surface. Meanwhile, the different types of vegetable oil and mass fraction of the nano-enhancers also had a significant effect on defect inhibition.

3.1.6 Analysis of the grinding defects and solutions

According to the research results, the grinding defects and bottlenecks of titanium alloy can be summarised as follows:

(i) Deterioration of the tribological properties caused by low elastic modulus. The elastic modulus of titanium alloy is 114 GPa, which is about 60% of the nickel-based alloy and high-strength steel. The abrasive removes material with negative rake cutting, giving the grinding force the appearance of ‘high pressure and low shear’. Then, the high pressure caused titanium alloy to rebound and retreat, resulting in vibration and surface roughness reduction during the grinding. In this case, the ratio of friction energy to grinding energy is higher than the other materials, which not only produces more friction heat but also intensifies the abrasive wear.

(ii) Deterioration of the workpiece surface integrity caused by low thermal conductivity. The heat transfer outlet in the grinding zone includes: workpiece, abrasive, lubricants, debris, and air. In titanium alloy grinding, the energy transmitted into the workpiece can reach more than 58% of the total energy [102,103]. However, the heat cannot be quickly transmitted through the matrix due to the low thermal conductivity of the titanium alloy, thus accumulating on the workpiece surface. At present, studies have confirmed that grinding defects caused by heat accumulation include the following aspects: ① Grinding burn and crack. The grinding burn is the black area that can be observed on the workpiece surface. ② Material adhesion on the workpiece. Adhesion occurs when the material is crushed to the surface of the workpiece by the abrasive as a result of thermal softening

at high temperature. ③ Ploughing and plastic uplift. The plastic ploughing phenomenon is intensified, and the material removal rate is decreased under the thermal softening effect. Thus, more materials are accumulating on both sides of the furrow.

According to the grinding experimental results, the bottleneck in ② has a stronger effect on the machining results than that in ①. Currently, scholars focus on improving the heat transfer capacity of lubricants and reducing the energy proportion that flows into the workpiece. The current research methods and conclusions are shown in Table 3 [89–93,96,102], which can be summarised as follows:

(i) Graphene with high thermal conductivity was used as a nano-enhancer to prepare the nano-enhanced biolubricant with palm oil, which had better heat exchange and antifriction performance, and achieved the best grinding experimental results compared with the other lubricants.

(ii) Combining cryogenic air and nano-enhanced biolubricant can significantly improve the heat transfer performance, which has been verified by preliminary experiments. This approach is one of the powerful techniques to solve the problem of titanium alloy grinding.

3.2 Nickel-based alloy

Nickel-based alloy has high strength and certain oxidation corrosion resistance at 650–1000 °C. The nickel-based alloy types for aerospace applications include Inconel series (718, 600, 625, etc.) and Incoloy series (825, A-286, etc.). This type of alloy is mainly used in the heat resistant parts of aeroengines, turbine blades, space shuttle engines, gas turbines and so on. Apart from the low thermal conductivity, the high hardness of nickel-based alloys is a source of grinding bottlenecks, distinguishing them from titanium alloys and high-strength steels [104–106]. The chemical composition and mechanical properties of the commonly used Inconel 718 are shown in Tables 4 and 5.

Table 3 Grinding conditions and experimental results of titanium alloy [89–93,96,102]

Ref.	Lubricant	Nano-enhancer	Workpiece	Evaluation parameters	Conclusion
[89]	Vegetable oil, synthetic esters	–	Ti–6Al–4V	Force, surface roughness, and workpiece surface topography	Synthetic esters > vegetable oil > soluble oil
[90]	Vegetable oil	Graphene	Ti–6Al–4V	Force, CoF, grinding temperature, surface roughness, microhardness, and workpiece surface topography	Graphene MQL > vegetable oil MQL > dry grinding
[91]	Palm oil, synthetic esters	Graphene	Ti–6Al–4V	Force, CoF, specific grinding energy, surface roughness, and workpiece surface topography	Optimal graphene concentration is 0.1 wt.%. Canola oil is optimal
[92]	Canola oil, soybean oil, olive oil	Graphene Graphite	Ti–6Al–4VELI	Force and workpiece surface topography	
[93]	Water	MoS ₂ Al ₂ O ₃	Ti–6Al–4V	CoF, workpiece surface topography, EDS of workpiece, wheel wear, debris morphology, and surface roughness	Al ₂ O ₃ MQL > water MQL
[96]	Synthetic esters	–	Ti–6Al–4V	Material removal rate and grinding temperature	MQL material removal rate is higher than flood
[102]	Synthetic esters	Al ₂ O ₃	Ti–6Al–4V	Debris morphology	Al ₂ O ₃ MQL > synthetic esters MQL > dry grinding

3.2.1 Force and CoF

Viridi et al. [107,108] used sunflower, rice bran, palm, and peanut oil in the MQL grinding experiment of Inconel 718. They found that the usage of biolubricant significantly reduced the CoF compared with flood, whilst the force, specific grinding energy and temperature are inferior to flood, as shown in Fig. 9 [107–110]. Amongst the four types of biolubricants, palm oil obtained the best experimental results, with the specific grinding energy and CoF reduced by 2.5% and 25.0% compared with flood, respectively.

Based on the above research, palm oil has achieved excellent lubrication performance amongst the various vegetable oils, and the reasons can be summarised into

two aspects: ① Palmitic acid (C16:0, 35%–48%), the main fatty acid component of palm oil, is saturated fatty acid. Meanwhile, the component of sunflower, peanut and rice bran oil (oleic acid, linoleic acid, etc.) is unsaturated fatty acid. ② Palm oil showed a higher viscosity value, reaching 38 mPa·s at 40 °C.

Wang et al. [109] compared the MQL grinding performance of the various vegetable lubricants (castor, soybean, rapeseed, corn, peanut, palm, and sunflower oil) for grinding of Inconel 718. Castor oil achieved the minimum normal and tangential grinding forces ($F_n = 76.83$ N, $F_t = 24.33$ N). The unique advantages over the other vegetable oils are as follows: ① Ricinoleic acid (C18:1), the main component of castor oil, contains a polar group –OH, which significantly enhances the adsorption strength of the lubricating oil film at the interface. ② The viscosity of castor oil is one order of magnitude higher than that of other vegetable oils, reaching 260 mPa·s at 40 °C. This condition is beneficial to the improvement of the tribological characteristics. However, the high viscosity of castor oil results in an increase in the grinding temperature, which was mentioned in the study of Li et al. [110] and will be discussed in detail later. Zhang et al. [111] also found that in the grinding of the nano-enhanced biolubricant prepared by Al₂O₃/SiC nano-enhancers with palm oil and castor oil, the grinding force obtained with palm oil as base oil is less than that obtained with castor oil.

Viridi et al. [108] observed the reduction of CoF and specific grinding energy with 17.7% and 29.4% respectively in grinding Inconel 718 with palm oil/Al₂O₃

Table 4 Chemical composition of Inconel 718

Chemical composition	Mass ratio/wt.%
Al	0.95
Mn	0.35
Fe	Balance
Cr	18.80
Cu	0.30
Ni	53.40
Co	1.00
Mo	2.99
Si	0.35
C	0.08

Table 5 Mechanical properties of Inconel 718

Material	Hardness	Yield strength	Elongation	Tensile strength	Elasticity modulus	Density	Thermal conductivity	Specific heat
Inconel 718	100 HRC	550 MPa	45%	965 MPa	199.9 GPa	8.24 g/cm ³	14.7 W/(m·K)	435 J/(kg·K)

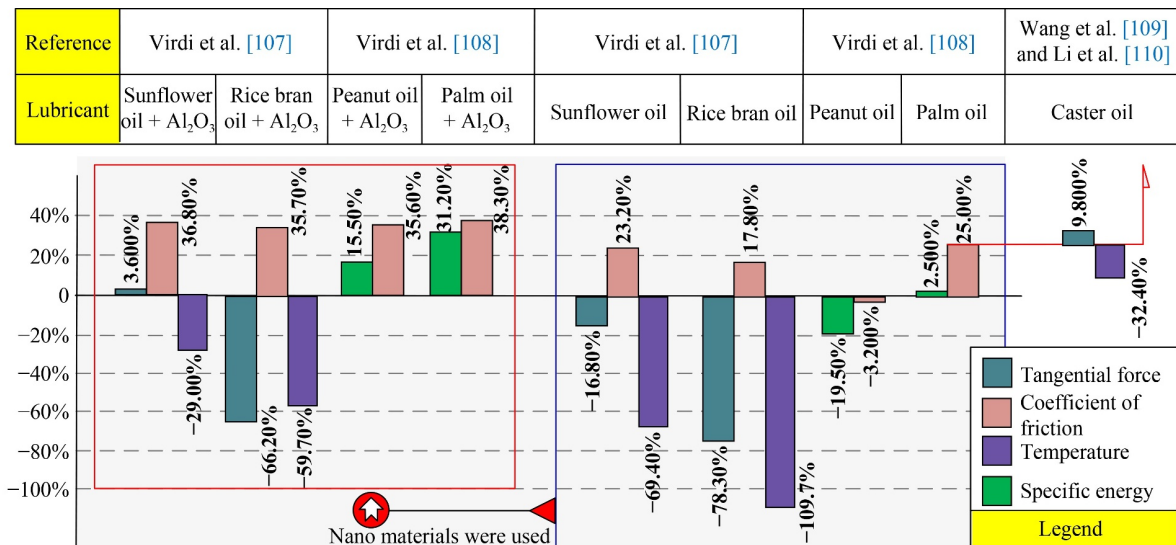


Fig. 9 Improvement ratio of biolubricant MQL compared with the traditional conditions [107–110].

NMQL compared with biolubricant. When sunflower oil/ Al_2O_3 was used in NMQL, the normal and tangential grinding forces decreased by 4.15% and 17.50%, respectively. The CoF decreased from 0.142 to 0.117, and the specific grinding energy decreased from 39.542 to 32.901 J/mm^3 [107]. In the NMQL experiment conducted by Wang et al. [112], the different performances of Al_2O_3 and MoS_2 were compared. The CoF decreased from 0.45 to 0.40 in palm oil/ MoS_2 NMQL and 0.38 in palm oil/ Al_2O_3 NMQL compared with MQL. Spherical Al_2O_3 has high hardness and plays a supporting role between the wheel and the workpiece, thus reducing the actual contact area of the friction pair. The rolling effect is produced on the uneven surface of the workpiece when it enters the grinding zone; accordingly, the sliding friction is transformed into rolling friction to produce an antiwear effect, which can reduce the tangential force and CoF. Zhang et al. [113] used synthetic ester to prepare the coolant with carbon nano tubes (CNTs), MoS_2 , and hybrid nano-enhancer CNTs/ MoS_2 . The experiment of grinding Inconel 718 showed that hybrid nano-enhancers exhibited stronger cooling and lubrication performance compared with a single one. These two nano-enhancers with different structures can improve the lubrication state of the grinding zone through physical synergy, and the grinding force is significantly reduced. The addition of different forms of nano-enhancers has different abilities of improving the cooling and lubrication performance. Spherical and layered nano-enhancers are more favourable for antifriction and antiwear but have lower thermal conductivity. Meanwhile, tubular CNTs have higher thermal conductivity and heat transfer capacity, but they are not conducive to lubrication. Zhang et al. [114] used vegetable oil combined with Al_2O_3 , SiC, and $\text{Al}_2\text{O}_3/\text{SiC}$ hybrid nano-enhancers for grinding Inconel 718. The grinding forces are $F_n = 84.91$ N, $F_t = 25.31$ N (Al_2O_3), and $F_n = 93.21$ N; $F_t = 30.81$ N (SiC) when single nano-enhancers are used, whilst the forces are $F_n = 70.91$ N; $F_t = 20.03$ N when hybrid nano-enhancers are used. The specific grinding energy of the hybrid nano-enhancers is reduced by 20.9% and 34.9% compared with Al_2O_3 and SiC NMQL, respectively, which is consistent with the experimental results of Zhang et al. [113]. Zhang et al. [115] evaluated the effect of the different particle sizes of hybrid nano-enhancers on the grinding force. They found that the grinding force reached the smallest when the particle size ratio of Al_2O_3 and SiC was 7:3.

Wang et al. [116] found that the specific grinding energy showed a trend of decreasing first and then increasing with the increase in Al_2O_3 concentration. At 1.5 vol.%, the specific grinding energy reached the minimum value (64.95 J/mm^3), which was 34.1% lower than that of pure oil. Accordingly, the proper concentration can improve the tribological properties, whilst a considerably high one will lead to aggregation,

which is not conducive to the tribological properties. Li et al. [117] obtained similar results in Inconel 718 grinding with palm oil/CNT.

3.2.2 Wheel wear

Severe wear and short service life of wheel are the main technical bottlenecks in the grinding process of nickel-based alloy. Viridi et al. [108] evaluated wheel wear using different biolubricants in MQL grinding of Inconel 718. The G-ratio increased by 50.60% when palm oil was used compared with peanut oil. In the other experiment, the G-ratio in sunflower oil increased by 3.61% compared with rice bran oil [107]. This result is obtained because the viscosity of sunflower oil is higher than that of rice bran oil, reducing the fluidity and prolonging the lubrication time of the grinding interface, thus preventing wheel wear. The life rule of wheel with different vegetable oil is consistent with grinding force, which depends on the lubrication performance. When Al_2O_3 was added to the sunflower oil, the G-ratio increased from 0.688 to 1.532. The abrasive was protected from wear due to the stable lubricating oil film formed by the nano-enhanced biolubricant. In addition, the G-ratio was significantly increased by increasing the concentration of the nano-enhancers. Hegab et al. [118] found that wheel wear was significantly improved with the addition of nano-enhancers in grinding Inconel 718. This phenomenon is mainly attributed to nano-enhancers that improve the lubrication and wettability in rake face/debris and back face/machined workpiece interfaces, thus improving the wear behaviour. Moreover, the wear decreases by 26.3% when multi-walled carbon nano tube (MWCNT) was used compared with Al_2O_3 . Wang et al. [109] carried out a series of experiments and reached a consistent conclusion. In comparison with the grinding performance of the different biolubricants, the different molecular structure, carbon chain length and other factors have different effects on the G-ratio.

When Inconel 718 was machined with palm oil/ MoS_2 and palm oil/ Al_2O_3 , the addition of nano-enhancer increased the G-ratio. NMQL increased the G-ratio by 23.9% and 32.9% compared with palm oil. Different types of nano-enhancers improved the G-ratio to varying degrees [112]. However, in the study of the effect of different volume fractions of Al_2O_3 on wheel wear, the G-ratio shows a trend of increasing first and then decreasing with the increase of volume fraction and reaches the maximum at 2.5 vol.% [116]. The SEM and EDS analysis of the abrasive showed that a micro-storage layer similar to the capillary on the wheel surface can temporarily store nano-enhanced biolubricant and effectively bring it into the grinding zone. Meanwhile, spherical Al_2O_3 plays a good bearing role in the grinding zone, changing the sliding friction between the abrasive

and the workpiece into rolling friction. Spherical Al_2O_3 reduced the wear plane of abrasive by reducing the contact area between the abrasive and the workpiece (Fig. 10 [116]).

3.2.3 Grinding temperature

The corundum wheel and CBN superhard abrasive wheel are mostly used in grinding nickel-based alloy. However, the biggest problem is the adhesion blockage of the grinding wheel. The nickel-based alloy with low thermal conductivity generates a large amount of heat and concentrates on the workpiece surface during material removal, resulting in the increase in the grinding temperature. Thermal damage caused by high grinding temperature seriously affects the workpiece quality and limits the production efficiency. Therefore, the effective heat transfer of lubricant is one of the important factors.

In Inconel 718 grinding experiment of Viridi et al. [107], the grinding temperature of sunflower oil MQL was 19.2% lower than that of rice bran oil MQL (Fig. 9 [107–110]). After Al_2O_3 nano-enhancers were added into the sunflower oil, the grinding temperature was further reduced from 105 to 80 °C. Li et al. [110] compared the grinding temperatures of castor, soybean, rapeseed, corn, peanut, palm and sunflower oil MQL in the grinding experiment of Inconel 718. They found that palm oil MQL reached the minimum value (119.6 °C), and castor oil MQL reached the maximum value (176.0 °C). This result is different from that of grinding force. The fundamental reason is that the physicochemical properties

of vegetable oil have different influencing trends on the lubrication and cooling performance: ① The fluidity of the vegetable oil molecules is poor in the heat transfer process because castor oil contains $-\text{OH}$ and present high viscosity, thus resulting in lower heat transfer efficiency. ② Although castor oil obtained the lowest grinding force (i.e., the minimum heat output) in the study of Wang et al. [112], the reduced heat transfer efficiency still resulted in the energy transmitted to the workpiece reaching the maximum value amongst various oils. ③ Palm oil is used as a lubricant with moderate viscosity to achieve a minimum grinding temperature. Zhang et al. [119] also found that surface tension had a significant impact on heat transfer performance, mainly because it affected the particle size and spread area of the microdroplets, thus changing the effective heat transfer area of lubricant.

Li et al. [120] added nano-enhancers into the palm oil and significantly improved the heat transfer performance. The effects of the different nano-enhancers (MoS_2 , SiO_2 , PCD, CNT, Al_2O_3 , and ZrO_2) on the grinding temperature were also compared. The thermal conductivity of CNT was the highest, resulting in the lowest grinding temperature under the condition of CNT nano-enhanced biolubricants. In the palm oil/CNT experiment with different concentrations, the concentration should not be considerably high or low, and an appropriate concentration can reduce the grinding zone temperature [117].

3.2.4 Debris morphology

Wang et al. [121] observed the debris morphology in the

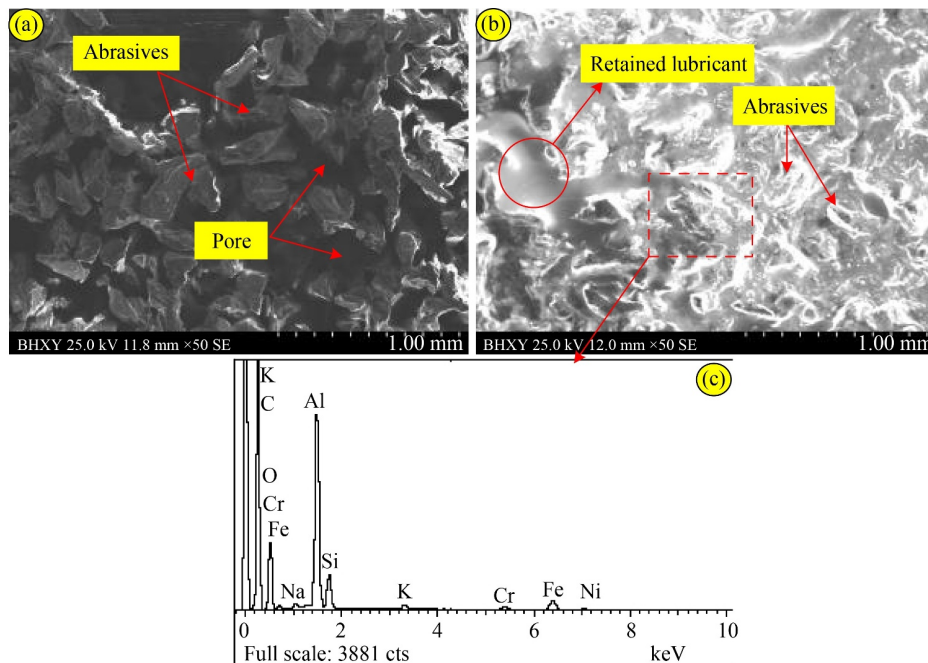


Fig. 10 Morphology and EDS analysis of the grinding wheel: (a) before grinding, (b) after grinding, and (c) EDS analysis. Reproduced with permission from Ref. [116] from Elsevier.

Inconel 718 grinding experiment (Fig. 11). The debris morphology under the MQL condition was longer and narrower compared with flood, and the surface was smoother. Furthermore, the debris under the palm oil/ Al_2O_3 NMQL condition are thinner compared with palm oil MQL, which is determined by the excellent lubrication performance of nano-enhancers. The debris can be well adsorbed in the texture of the debris surface or the grooves of the workpiece surface and act as rolling bearings to reduce friction between abrasive and debris [112]. Moreover, when the volume concentration of the Al_2O_3 nano-enhanced biolubricant reached 2 vol.%, the surface of the debris is smooth, and the strip debris with uniform width are presented. The change of debris morphology reflects the material removal mechanism, and the excellent lubrication performance plays an important role [116].

3.2.5 Surface integrity

According to Viridi et al.'s [107] grinding experiment of Inconel 718 using sunflower and rice bran oil, as shown in Fig. 12 [107,116,122], the surface roughness of both biolubricants can be reduced compared with flood. However, Ra in sunflower oil MQL also decreased by 5.49% compared with rice bran oil. When Al_2O_3 nano-enhancers were added, sunflower oil/ Al_2O_3 NMQL decreased by 41.90% compared with MQL.

Wang et al. [109] evaluated the surface quality in Inconel 718 grinding using different biolubricants. Castor oil reached the lowest surface roughness value of $0.36 \mu\text{m}$ due to its high viscosity, and the optimal workpiece surface was also obtained. Furthermore, MoS_2 and Al_2O_3

were used to prepare nano-enhanced biolubricants with palm oil. The addition of both nano-enhancers reduced the Ra values compared with palm oil. However, the Ra value of the Al_2O_3 nano-enhancers decreases by 13.3% compared with MoS_2 [112]. Li et al. [120] studied the surface quality considering the influence of the various nano-enhancers and found that nanodiamond has more advantages than others. Wang et al. [116] found that the surface quality when the volume concentration reaches 2% is the best (Fig. 12 [107,116,122]) using palm oil/ Al_2O_3 . The Al element content increase on the workpiece surface was also observed through EDS analysis. Li et al. [123] also obtained the same conclusion.

Zhang et al. [124] used CNTs/ MoS_2 hybrid nano-enhancers in the NMQL grinding of Inconel 718. The surface roughness obtained by hybrid nano-enhancers decreased by a maximum value of 85.3% compared with single nano-enhancer. This finding is consistent with the effect produced by grinding forces. Zhang et al. [114] also obtained the same conclusion in his experiment.

Viridi et al. [107] observed the workpiece surface topography and found the sliding and ploughing phenomena exist in almost all conditions, and some of them also have deep gullies and adhesion. In flood condition, severe ploughing and adhesion lead to poor workpiece surface integrity, and adhesion further aggravates the friction between grinding wheel and workpiece. The surface quality of vegetable oil was improved. However, slight stacking of materials, adhesion and wear marks caused by ploughing and accumulation were also observed. This phenomenon is due to the viscosity of vegetable oil that more slowly

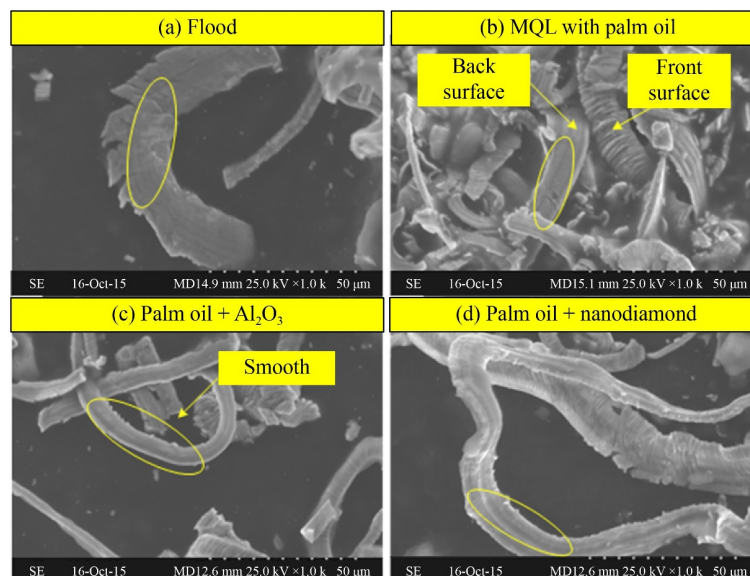


Fig. 11 Debris morphology under different lubrication conditions: (a) flood, (b) MQL with palm oil, (c) palm oil + Al_2O_3 , and (d) palm oil + nanodiamond. Reproduced with permission from Ref. [121] from Elsevier.

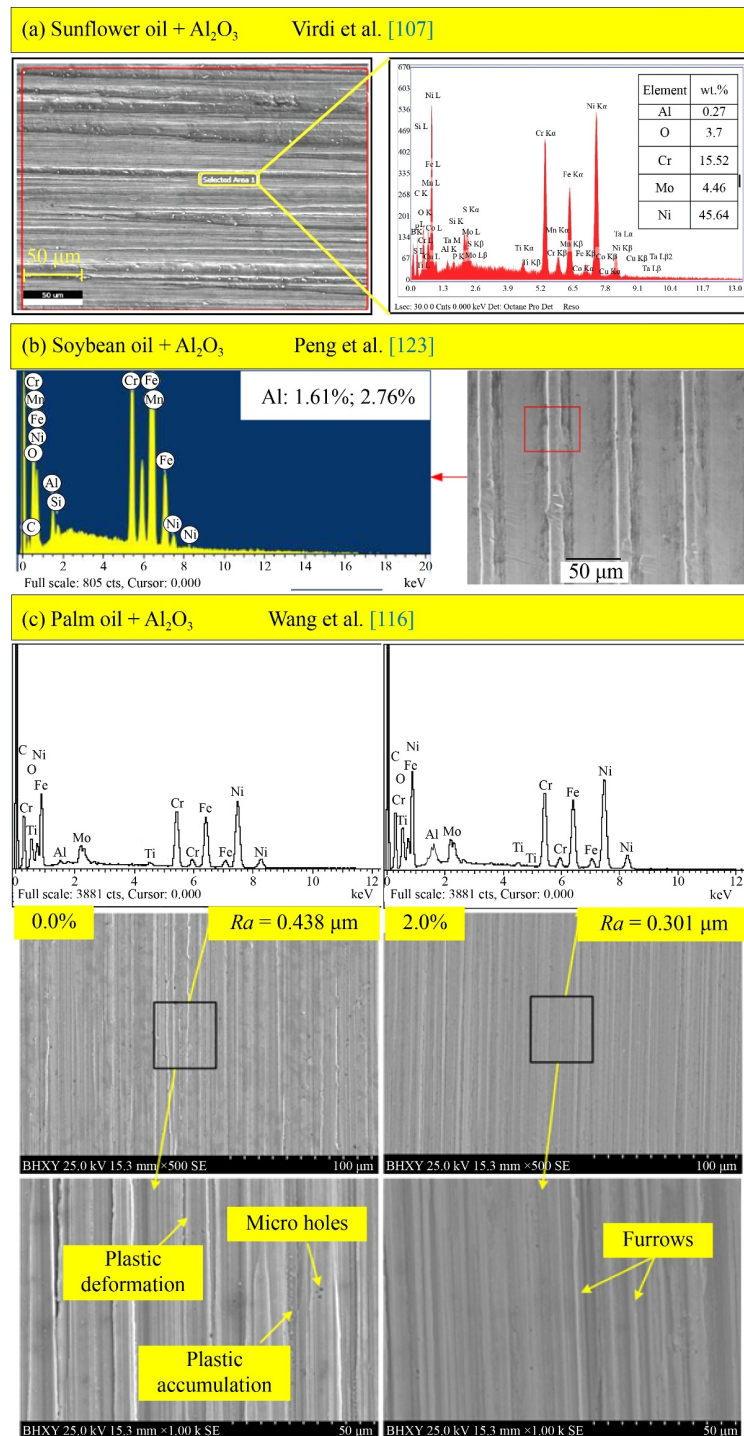


Fig. 12 Surface SEM and EDS analysis of Ni-based alloy using Al₂O₃ biolubricant: (a) sunflower oil + Al₂O₃ [107], (b) soybean oil + Al₂O₃ [122], and (c) palm oil + Al₂O₃ [116]. Reproduced with permission from Refs. [107,116,122] from Elsevier.

declines than that of mineral oil at higher temperatures. Accordingly, the higher viscosity ensures that the vegetable oil could provide more stable lubricity at the operating temperature range. Furthermore, the smoother surfaces, small number of narrower furrows and slight accumulation of plough are revealed under NMQL. The EDS analysis also confirmed the existence of a

lubricating oil film on the workpiece surface. Peng et al. [122] found an oxygen element on the workpiece surface in the grinding experiment of Inconel 718 using soybean oil/Al₂O₃ NMQL. This phenomenon was attributed to the chemical reaction and the formation of a lubricating oil film, which effectively improved the lubrication condition of grinding.

3.2.6 Analysis of grinding defects and solutions

According to the above-mentioned results, the grinding defects and bottlenecks of the nickel-based alloy can be summarised as follows.

(i) Wheel wear is aggravated due to high hardness. The hardness of nickel-based alloys reaches about 100 HRC, which is three to five times bigger than titanium alloys and high-strength steels. The high hardness comes from the following reasons: ① The high melting point alloying elements of the nickel-based alloys (nickel, iron, chromium, etc.) combine with other elements to form high-hardness materials, such as austenitic alloys, high-hardness compounds, high-hardness intermetallic compounds, and hard particles. ② Nickel-based alloy is treated with a solution treatment before machining, and work hardening occurs in the process, resulting in the increase of hardness. ③ After aging treatment, the hard phase in the solid solution is precipitated, and the lattice is distorted, resulting in aging strengthening.

In grinding, bottlenecks caused by high hardness are as follows: ① The interference area between abrasive and debris decreases due to the low plastic deformation

degree of the workpiece in the abrasive material removal, which results in the increase of the unit mechanical/thermal load of the effective abrasive region and the aggravation of abrasive wear. ② The interference between hard phase and abrasive also aggravates abrasive wear. Therefore, scholars also focus on the wheel wear, G-ratio and other parameters.

(ii) Surface burns caused by low thermal conductivity. At 100 °C, the thermal conductivity of the nickel-based alloy is 14.7 W/(m·K). Although the conductivity of nickel-based alloy is higher than that of titanium alloy, some problems continue to persist, such as burn, furrow and plastic accumulation on the workpiece surface. However, the experimental results showed that such defects do not reach the severity of titanium alloy.

Accordingly, the lubricant should first meet the characteristics of antiwear and antifricition, whilst having a certain heat exchange capacity. The current research methods and conclusions are shown in Table 6 [107–124], which can be summarised as follows:

(i) The biolubricant should have high viscosity, fatty acid saturation, containing polar groups and other characteristics (e.g., palm oil and castor oil), which is

Table 6 Grinding conditions and experimental results of Inconel 718 [107–124]

Ref.	Lubricant	Nano-enhancer	Evaluation parameters	Conclusions
[107]	Sunflower oil and rice bran oil	Al ₂ O ₃	Force, CoF, specific grinding energy, G-ratio, grinding temperature, surface roughness, and workpiece surface topography	1. Sunflower oil > rice bran oil 2. Under Al ₂ O ₃ NMQL, optimal results are obtained
[108]	Peanut oil and palm oil	Al ₂ O ₃	CoF, specific grinding energy, and G-ratio	1. Palm oil > peanut oil > flood 2. Al ₂ O ₃ NMQL > MQL
[109]	Paraffin, soybean oil, peanut oil, corn oil, rapeseed oil, palm oil, castor oil, and sunflower oil	–	CoF, specific grinding energy, G-ratio, surface roughness, and workpiece surface topography	1. Vegetable oil > paraffin 2. Castor oil is the best
[110]	Castor oil, soybean oil, rapeseed oil, corn oil, peanut oil, palm oil, and sunflower oil	–	Force and grinding temperature	1. Castor oil has the lowest force 2. Palm oil has the lowest grinding temperature, and castor oil has the highest
[111]	Palm oil and castor oil	Al ₂ O ₃ + SiC	Force, specific grinding energy, and surface roughness	Palm oil > castor oil
[112]	Palm oil	Al ₂ O ₃ , MoS ₂	CoF, specific grinding energy, G-ratio, debris, surface roughness, and workpiece surface topography	Al ₂ O ₃ NMQL > MoS ₂ NMQL > palm oil MQL
[113]	Synthetic esters	CNT, MoS ₂	Force	Hybrid nano-enhancers > single nano-enhancer
[114]	Vegetable oil	Al ₂ O ₃ , SiC	Force	Hybrid nano-enhancers > single nano-enhancer
[115]	Vegetable oil	Al ₂ O ₃ , SiC	Force	Optimal particle size ratio is Al ₂ O ₃ :SiC = 7:3
[116]	Palm oil	Al ₂ O ₃	Specific grinding energy, G-ratio, debris, and workpiece surface topography	1. Optimal Al ₂ O ₃ concentration (specific grinding energy) is 1.5 vol.% 2. Optimal Al ₂ O ₃ concentration (G-ratio) is 2.5 vol.%
[117]	Palm oil	CNT	Force and grinding temperature	Optimal CNT concentration is 2 vol.%
[118]	Vegetable oil	MWCNT and Al ₂ O ₃	Wheel wear	MWCNT NMQL > Al ₂ O ₃ NMQL
[119]	Liquid paraffin, palm oil, rapeseed oil, and soybean oil	MoS ₂	Force, CoF, and specific grinding energy	Palm oil is the optimum base oil of MQL
[120]	Palm oil	MoS ₂ , SiO ₂ , PCD, CNT, Al ₂ O ₃ , and ZrO ₂	Grinding temperature, surface roughness, and working surface topography	CNT NMQL is optimal
[121]	Palm oil	Al ₂ O ₃	Debris morphology	Al ₂ O ₃ NMQL > palm oil MQL > flood
[122]	Soybean oil	Al ₂ O ₃	Surface roughness and workpiece surface topography	Optimal Al ₂ O ₃ concentration is 2 wt.%
[123]	Palm oil	CNT	Workpiece surface topography	Optimal CNT concentration is 2 vol.%
[124]	Synthetic esters	Al ₂ O ₃ , MoS ₂	Surface roughness	Hybrid nano-enhancers > single nano-enhancer

conductive to the formation of strong adsorption of a lubricating oil film. Nano-enhancers should have high hardness and spherical characteristics (e.g., Al_2O_3); thus, they play an excellent role of rolling antifriction and antiwear in a high-pressure grinding interface.

(ii) The recommended nano-enhancers have low thermal conductivity. To give consideration to the heat transfer capacity and solve the grinding burn phenomenon, the use of hybrid nano-enhancers is one of the feasible solutions. The commonly used nano-enhancers with high thermal conductivity include CNTs and SiC.

3.3 High-strength steel

High-strength steel (AISI 4140, 4340, 52100, etc.) plays an important role in the aerospace field because of its high tensile strength. The applications include rocket engine housing, aircraft landing gear, bulletproof steel plate and other parts with special performance requirements. Given that the yield and tensile strength of high-strength steel are higher than those of titanium and nickel-based alloys, it is difficult to be removed and form debris in grinding. Wheel clogging and high grinding temperature lead to the surface layer of the workpiece changes, which is directly reflected in the changes of microhardness and residual stress [125,126]. The chemical composition and physicochemical properties of the commonly used high-strength steels are shown in Tables 7 and 8.

3.3.1 Force and CoF

Sadeghi et al. [127] used biolubricant and synthetic ester in the AISI 4140 grinding experiment, which significantly improved the performance compared with flood. Taking tangential grinding force as example, vegetable oil and synthetic ester were reduced by 57.2% and 67.5% compared with flood, respectively. Meanwhile, synthetic ester produced less grinding force compared with biolubricants, with 22.8% and 22.9% reduction in the normal and tangential directions, respectively (Fig. 13

[127–132]). In the AISI 1018 grinding experiment of Shao et al. [128], commercial vegetable oil was used in MQL, and the CoF was reduced from 0.299 to 0.271 compared with flood. The above conclusions are consistent with titanium alloy grinding and verify the advantages of synthetic ester. This finding is attributed to the introduction of polar groups in the preparation of synthetic ester, thus improving the adsorption capacity of the lubricating oil film. Mao et al. [129] also used water and water-based Al_2O_3 nanofluids in the AISI 52100 grinding experiment. In comparison with water-based MQL, the tangential force decreased by 10.92%, whilst the force ratio decreased by 11.11% with the addition of Al_2O_3 . Furthermore, Ref. [132] found that the use of canola oil/ MoS_2 nano-enhanced biolubricant achieved a lower grinding force compared with water/ Al_2O_3 . ManojKumar and Ghosh [130] used MWCNT and sunflower oil to prepare the coolant when they carried out the NMQL experiment of AISI 52100 grinding. In comparison with MQL, the specific grinding energy of sunflower oil/MWCNT NMQL decreased by 11.9%, and the force ratio decreased from 0.37 to 0.35. The addition of nano-enhancers increases the viscosity of the lubricant from 44.2 to 47.96 mPa·s, thus enhancing the lubrication performance. Molaie et al. [131] achieved smaller results with the addition of nano-enhancers than under MQL conditions when grinding AISI 52100 with pure water MQL and NMQL.

Molaie et al. [131] further compared the grinding performance of the nano-enhanced biolubricants prepared by pure water and four types of nano-enhancers, namely, Al_2O_3 , graphite, graphene oxide, and CNTs. The results showed that the grinding force of water/graphene oxide was the smallest ($F_n = 74.2$ N, $F_t = 26.3$ N). In the subsequent experiments, scholars mixed Al_2O_3 and graphite to prepare hybrid nano-enhanced biolubricants, and the grinding performance was improved, which is due to the different tribological mechanism of the two types of nano-enhancers. The layered structure of graphene oxide allows easy access to the sliding zone and reduces the direct contact between particle with the metal,

Table 7 Chemical composition of high-strength steels

Material	Mass ratio/wt. %							
	C	Mn	P	S	Cr	Mo	Si	Ni
AISI 4140	0.380–0.430	0.700–1.000	0.035	0.040	0.800–1.100	0.150–0.250	0.170–0.370	0.300
AISI 4340	0.380–0.430	0.600–0.800	0.035	0.040	0.700–0.900	0.200–0.300	0.150–0.350	1.650–2.000
AISI 52100	0.950–1.050	0.250–0.450	0.025	0.025	1.400–1.650	0.080	0.150–0.350	0.300

Table 8 Mechanical properties of high-strength steels

Material	Hardness/ HRC	Yield strength/MPa	Elongation/%	Tensile strength/MPa	Elasticity modulus/GPa	Density/ ($\text{g}\cdot\text{cm}^{-3}$)	Thermal conductivity/ ($\text{W}\cdot\text{m}^{-1}\cdot\text{K}^{-1}$)	Specific heat/ ($\text{J}\cdot\text{kg}^{-1}\cdot\text{K}^{-1}$)
AISI 4140	22.2	930	12	1080	185	7.85	46	0.27–0.30
AISI 4340	27.8	835	12	980	208	7.83	–	0.30

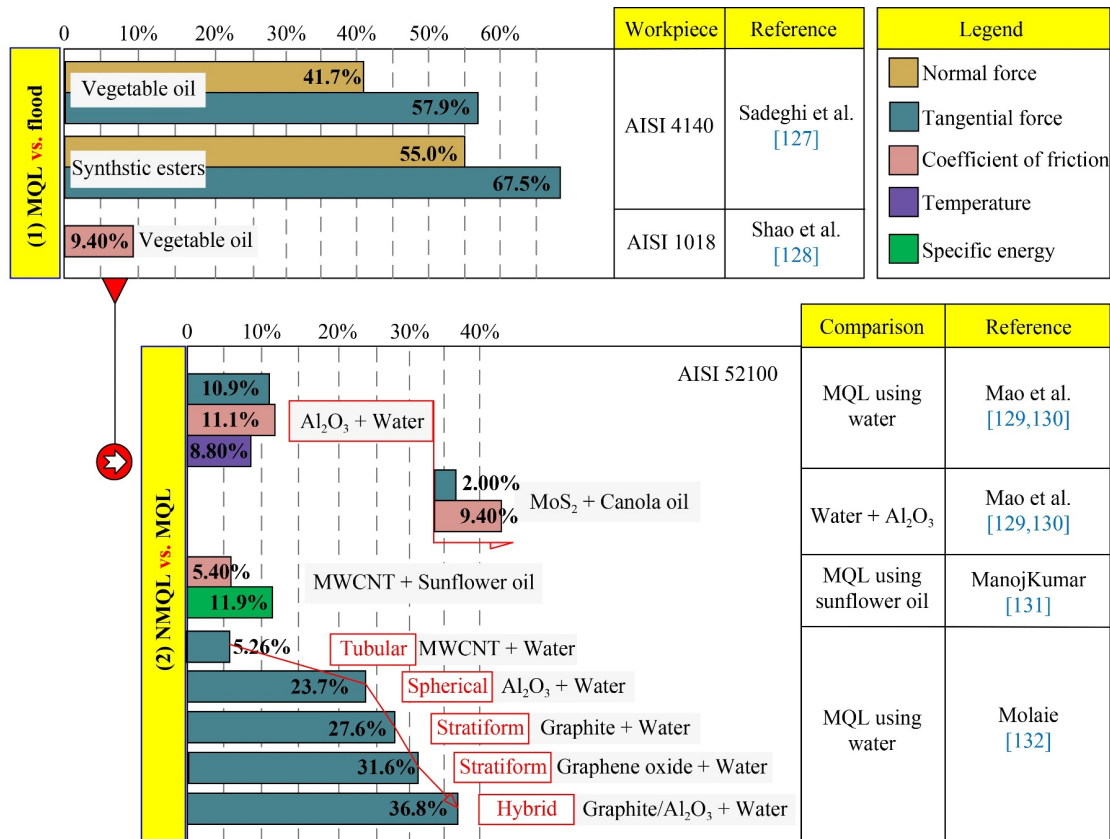


Fig. 13 Grinding performance of high-strength steel using biolubricant [127–132].

forming a protective and durable friction film. Meanwhile, spherical Al₂O₃ nano-enhancers with high hardness can produce a ball effect between friction surfaces.

3.3.2 Wheel wear

de Mello Belentani et al. [133] used flood, vegetable oil and vegetable oil/water mixture (mixing ratio 1:5) as lubricants in AISI 4340 grinding. The wheel wear rate was reduced under MQL compared with flood, as shown in Fig. 14 [133]. The wheel wear degree depends on the thermal/force boundary conditions in the grinding zone:

① The lack of lubrication ability under flood results in the aggravation of abrasive wear. ② Vegetable oil as lubricant still has a high wear rate because the high viscosity lubricant does not have the wheel washing performance, resulting in porosity blockage. ③ The above-mentioned problems can be addressed using vegetable oil/water mixture. The washing performance of the lubricant on the wheel is also enhanced with the increase in water proportion, and the wheel wear rate is lower. Javaroni et al. [134] used a cooled wheel cleaning jet (CWCJ) technology in combination with MQL to significantly optimise the wheel wear rate by using CWCJ's cleaning effect on the wheel. Moreover, the wheel wear rate further decreases with the decrease in

high-pressure gas temperature, as shown in Fig. 15 [134]. Garcia et al. [135] used a vegetable oil/water mixture (mixing ratio 1:5) as lubricant, and the wear rate was reduced by 33.3% when with a wheel cleaning jet (WCJ) technology in the AISI 52100 grinding experiment. Therefore, the wheel cleaning performance of the lubrication process is important to wheel life.

ManojKumar and Ghosh [130] employed soluble synthetic oil, sunflower oil and sunflower oil/MWCNT nano-enhanced biolubricant as the lubrication media in the grinding experiment of AISI 52100. The G-ratio of the three lubricants increased by 23.1%, 26.9%, and 69.2% compared with flood. The addition of nano-enhancers has a more prominent effect on wheel life.

3.3.3 Grinding temperature

Mao et al. [129] analysed the change of grinding temperature in the AISI 52100 grinding experiment. The grinding temperature after adding nano-enhancers (Al₂O₃) decreases from 484 to 442 °C, which decreases by 8.68%, compared with pure water MQL, as shown in Fig. 16 [129]. The reduction in the grinding temperature can also be verified by the workpiece microstructural distribution. The grinding surface after machining is composed of a white layer and a dark layer due to the influence of grinding heat, which have an impact on the service life

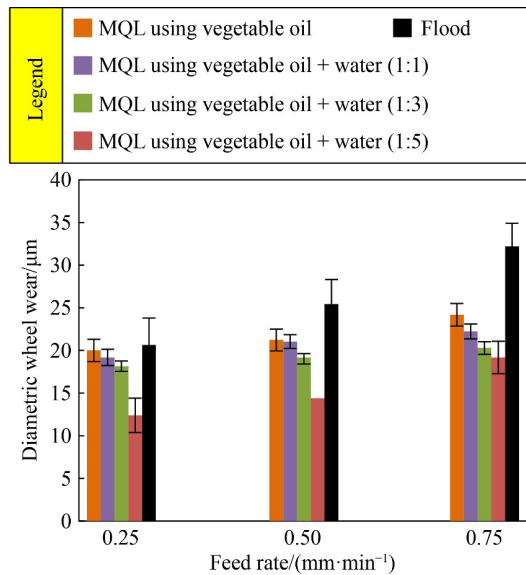


Fig. 14 Diametric wheel wear using vegetable oil + water hybrid lubricant [133].

and surface quality of the workpiece. The thicknesses of the white and dark layers are 8 and 32 μm when water is used as a lubrication medium, whilst 4 and 21 μm when water-based nanofluids are used, respectively. Therefore, the reduction of grinding temperature has a significant effect on the microstructural change of high-strength steel.

3.3.4 Debris morphology

Javaroni et al. [134] observed debris morphology of under flood, MQL and MQL + WCJ technologies. In flood, debris are strip and banding, indicating that debris formation is a ductile flow process (Fig. 17 [134]). In MQL, the debris is spherical. In the MQL + WCJ condition, the number of spherical debris is significantly lower than MQL, indicating that the cooling performance is stronger than MQL. Under the condition of MQL + WCJ (high-pressure gas with $-15\text{ }^{\circ}\text{C}$), the shape is similar to flood.

ManojKumar and Ghosh [130] observed the debris

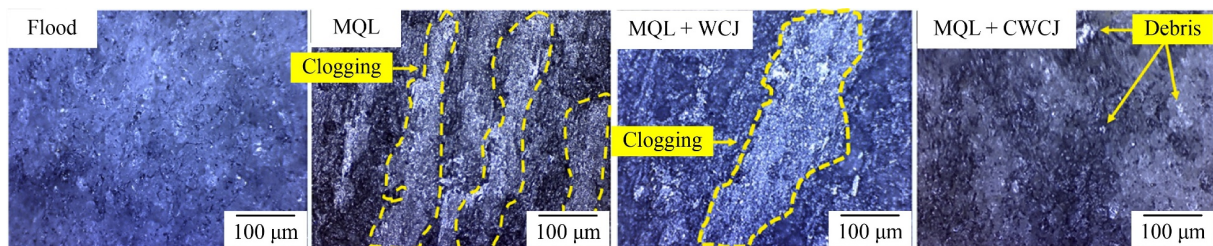


Fig. 15 SEM of the grinding wheel under different lubrication conditions. Reproduced with permission from Ref. [134] from Elsevier.

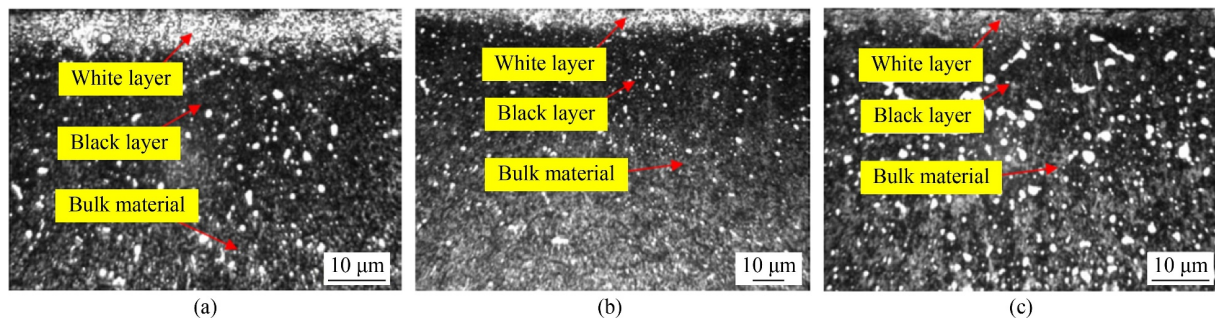


Fig. 16 Cross-sectional morphology under different lubrication conditions: (a) dry grinding, (b) MQL using water, and (c) MQL using water-based nano-lubricant. Reproduced with permission from Ref. [129] from Springer Nature.

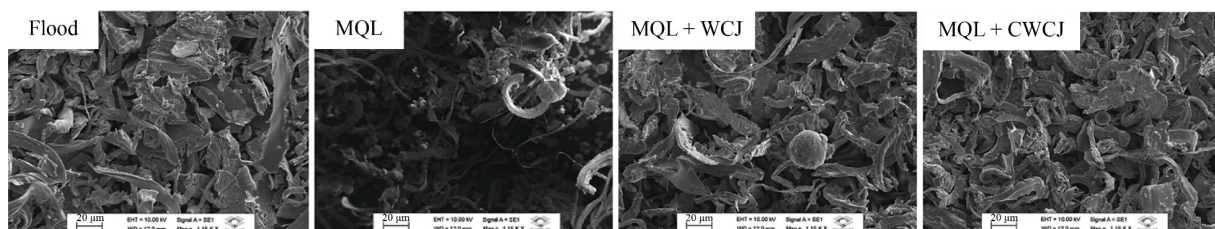


Fig. 17 Debris morphology under different lubrication conditions. Reproduced with permission from Ref. [134] from Elsevier.

morphology in the grinding experiment of AISI 52100 and found that the biolubricant MQL optimises the material removal process. A large number of elongated debris ① and a small number of weakly plastic deformation debris ② are present in sunflower oil condition, as shown in Fig. 18 [130]. In the case of sunflower oil/MWCNT, the number of weakly plastic deformation debris is small, and the debris is formed by cutting of the sharp abrasive, indicating that the nanofluids environment has better sharpness maintenance ability. When the lubricant flow is reduced, the number of strip debris increases. However, spherical debris were produced at the flow of 50 mL/h, indicating that the temperature in the grinding zone increased, which led to the melting and re-solidification of the debris material into a spherical shape. Therefore, the flow of the lubricant should be controlled in an appropriate range.

3.3.5 Surface integrity

Shao et al. [128] explored the distribution of residual stress on the AISI 1018 workpiece after grinding and found that residual compressive stress would be generated on the workpiece surface in MQL and flood conditions, whilst a higher residual tensile stress would be generated in dry conditions. ManojKumar and Ghosh [130] obtained the same rule in their experiments, as shown in Fig. 19 [130]. The residual compressive stress

was generated on the workpiece surface, which was due to the better reduction of the grinding temperature by nanofluids through reducing friction and enhancing thermal conductivity. The formation mechanism of the residual stress in the grinding process is complex, which is influenced by grinding heat and force: ① The grinding force results in the local plastic deformation of the workpiece and residual compressive stress on the surface. ② Thermal expansion and cold contraction also have a certain effect on the residual tensile stress, and the extremely high grinding temperature may induce phase transition and introduce residual stress.

Sadeghi et al. [127] compared the workpiece surface quality when grinding AISI 4140 with vegetable oil and synthetic ester MQL. They obtained a reduction of 19.0% in surface roughness under synthetic ester compared with vegetable oil MQL. The R_a value of these two biolubricants is lower than flood when the grinding depth is increased to 15 μm . This finding also fully proves that biolubricants are more advantageous in the case of large removal (high grinding force). Further observation of the surface and cross-section of the workpiece indicated that the surface using biolubricant is smoother, whilst burr and obvious plastic uplift are observed on the cross-section, as shown in Fig. 20 [127]. Mao et al. [129] added Al_2O_3 nano-enhancers in water when grinding AISI 52100, and the R_a value decreased by 38.71% compared with MQL. Nevertheless, a large number of plastic uplifts

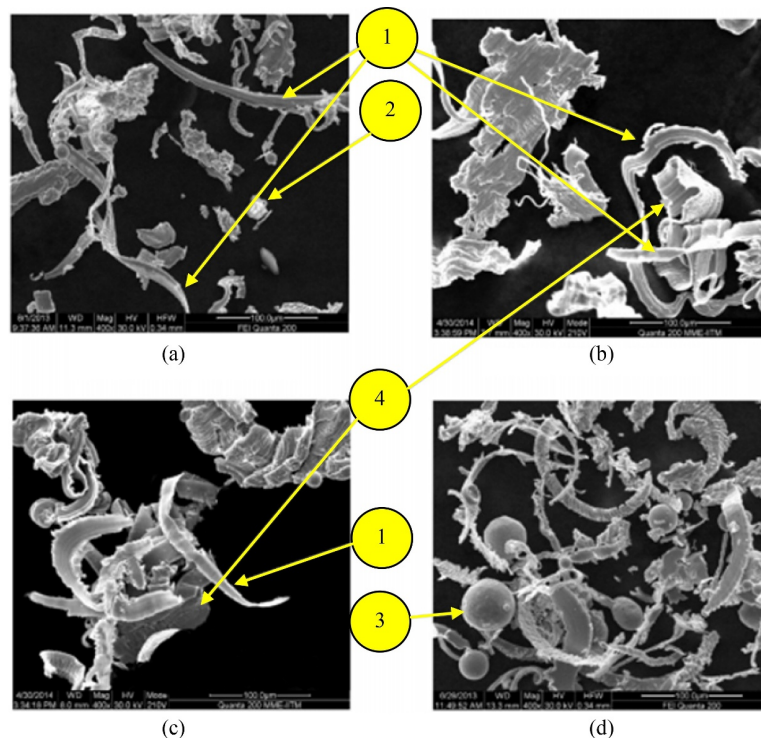


Fig. 18 Debris morphology under different lubricants and usage amounts: (a) sunflower oil, 500 mL/h, (b) sunflower oil + CNT, 500 mL/h, (c) sunflower oil + CNT, 200 mL/h, and (d) sunflower oil + CNT, 50 mL/h. Reproduced with permission from Ref. [130] from Elsevier.

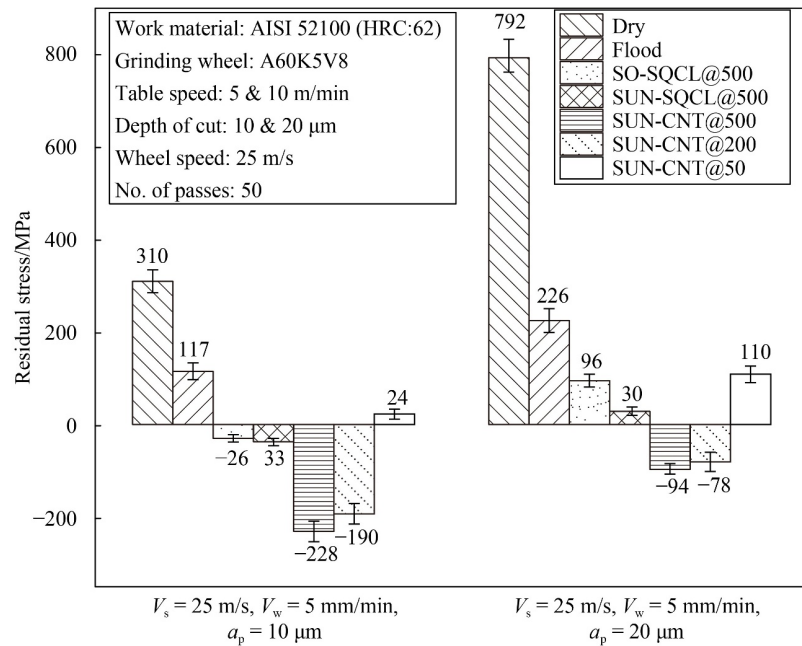


Fig. 19 Residual stress of workpiece under different lubrication conditions. Reproduced with permission from Ref. [130] from Elsevier.

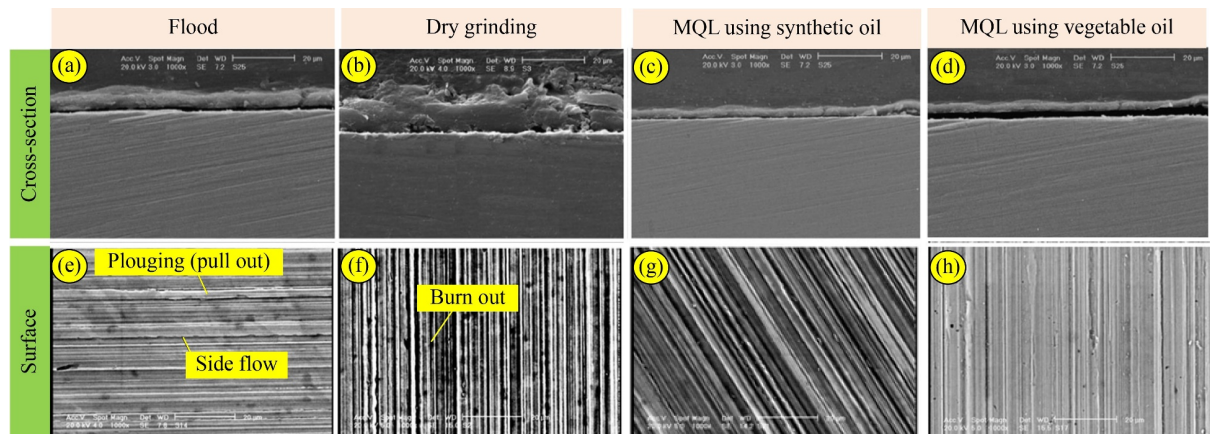


Fig. 20 Surface and cross-sectional morphology under different lubrication conditions. Cross-section: (a) flood, (b) dry grinding, (c) MQL using synthetic oil, and (d) MQL using vegetable oil. Surface: (e) flood, (f) dry grinding, (g) MQL using synthetic oil, and (h) MQL using vegetable oil. Reproduced with permission from Ref. [127] from Springer Nature.

were found on the workpiece surface. de Mello Belentani et al. [133] used vegetable oil mixed with water as lubricant (mixing ratio 1:5) to carry out the grinding experiment of AISI 4340, and the surface roughness decreased from 0.70 to 0.35 μm under the condition of vegetable oil. Molaie et al. [131] used four types of water-based NMQL (Al_2O_3 , graphite, graphene oxide, and MWCNT) conditions in AISI 52100 grinding. The surface roughness obtained by graphene oxide nano-enhanced biolubricants was the smallest ($R_a = 0.65 \mu\text{m}$) compared with pure water MQL ($R_a = 1.18 \mu\text{m}$).

Considering the flow rate of the biolubricant in AISI 4340 grinding, Javaroni et al. [136] found that surface quality was optimised with the increase in flow rate, and the plastic uplift and debris adhesion on the workpiece

surface were effectively avoided at 160 mL/h flow rate. The workpiece surface quality is further optimised when MQL and WCJ are used together as the biolubricant MQL has limited performance for wheel cleaning, as shown in Fig. 21 [136].

3.3.6 Analysis of grinding defects and solutions

According to above-mentioned results, the grinding defects and bottlenecks of high-strength steel can be summarised as follows:

(i) Wheel blockage caused by high strength. The tensile strength of high-strength steel is higher than that of titanium alloy and nickel-based alloy, which is difficult

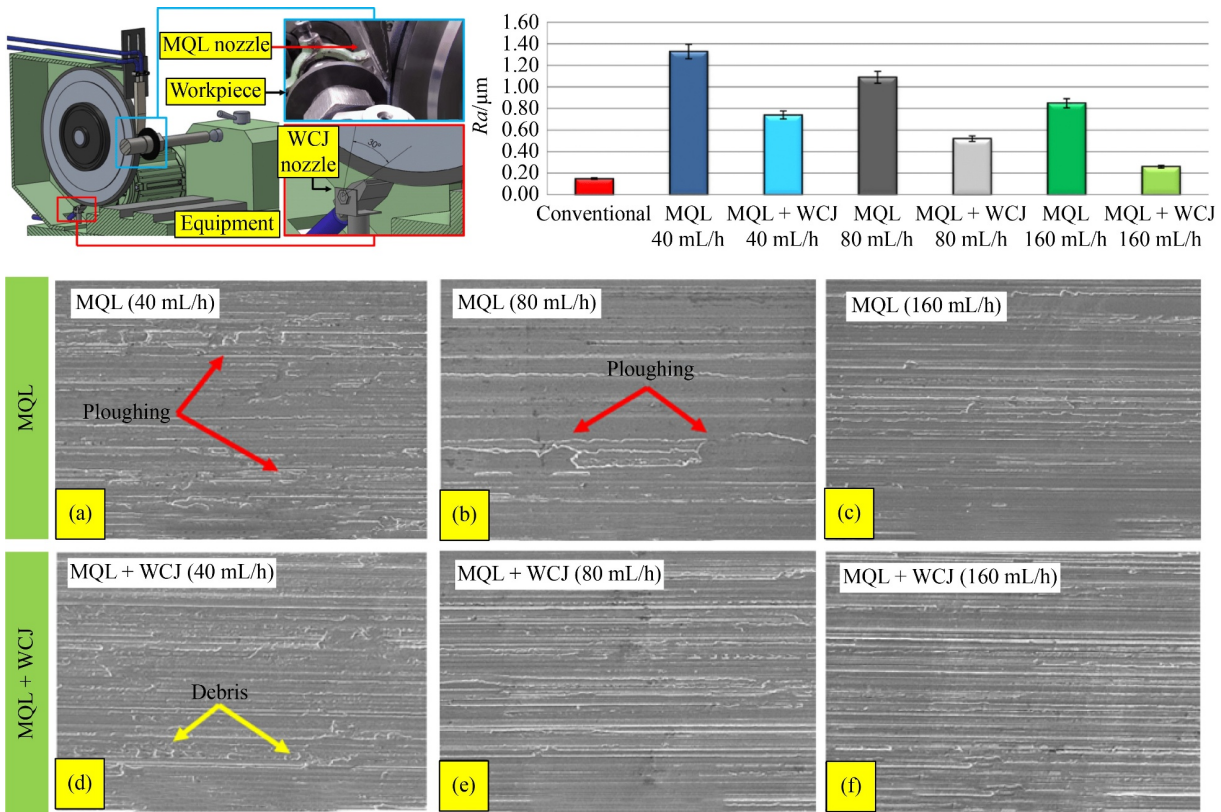


Fig. 21 Surface integrity under various usage amounts and with or without WCJ method: (a) MQL (40 mL/h), (b) MQL (80 mL/h), (c) MQL (160 mL/h), (d) MQL + WCJ (40 mL/h), (e) MQL + WCJ (80 mL/h), and (f) MQL + WCJ (160 mL/h). Reproduced with permission from Ref. [136] from Springer Nature.

for the material to deform after it is removed and formed into debris. The experimental results also showed that the deformation curvature of debris of high-strength steel is less than that of the other two materials. Accordingly, the discharge direction of debris is toward the wheel, and it is easy to accumulate in the wheel pore and cause the blockage, which is consistent with the observation that the wheel blockage is more serious than that of titanium alloy and nickel-based alloy. In addition, spherical debris is also found in the grinding of high-strength steel, which is due to the material melting caused by high temperature in the grinding zone. Part of the melted material is re-solidified as spherical debris and discharged from the cutting zone, whilst most will flow into the pore of the grinding wheel and cause serious blockage.

(ii) Microstructural transformation of the workpiece caused by high grinding temperature. The tribological characteristics deteriorate, and the grinding heat output increases due to the blockage of wheel and abrasive wear, resulting in a considerably high grinding temperature. Accordingly, this study confirmed that the material structure changes under the influence of high grinding temperature. Furthermore, the residual stress and microhardness of the workpiece will increase.

Therefore, the way to solve the grinding bottleneck of high-strength steel is to improve the cleaning

performance of the wheel and heat transfer performance of the grinding zone. The current research methods and conclusions are shown in Table 9 [127–136], which can be summarised as follows:

(i) Low viscosity biolubricants (canola oil and sunflower oil) have good fluidity and cleanliness compared with high viscosity lubricants and are more suitable for high-strength steel. The use of nano-enhancers can significantly improve the heat transfer performance, but there is no special requirement on the type and characteristics.

(ii) The wheel cleanliness of NMQL still needs to be improved. At present, the two feasible schemes are as follows: ① Using vegetable oil/water mixed lubricant to improve the grinding performance by reducing the lubricant viscosity and improving the thermal conductivity. ② The coupled use of WCJ or CWCJ with MQL also has an obvious effect.

4 Conclusions

In this review, a systematic review of MQL grinding of the aerospace materials with biolubricants was carried out. The mechanism of the biolubricant physicochemical property on the antifriction and antiwear, heat dissipation

Table 9 Grinding conditions and experimental results of high-strength steel [127–136]

Ref.	Lubricant	Nano-enhancer	Workpiece	Evaluation parameters	Conclusion
[127]	Vegetable oil, synthetic esters	–	AISI 4140	Force, surface roughness, microhardness, and workpiece surface topography	Synthetic esters > vegetable oil
[128]	Commercial vegetable oil	–	AISI 1018	CoF	Vegetable oil > flood
[129]	Water	Al ₂ O ₃	AISI 52100	Force, grinding temperature, surface roughness, and workpiece surface topography	Al ₂ O ₃ NMQL > water MQL
[130]	Sunflower oil	MWCNT	AISI 52100	Specific grinding energy, force ratio, and debris morphology	MWCNT NMQL > vegetable oil MQL
[131]	Water	Al ₂ O ₃ , graphite, graphene oxide, and CNTs	AISI 52100	Force and surface roughness	The optimal nano-enhancer is graphene oxide
[132]	Canola oil + water	MoS ₂ , Al ₂ O ₃	AISI 52100	Force	Canola oil/MoS ₂ NMQL > water/Al ₂ O ₃ NMQL
[133]	Vegetable oil + water	–	AISI 4340	Wheel wear and surface roughness	Vegetable oil MQL > flood
[134]	Vegetable oil	–	AISI 4340	Wheel wear and debris morphology	Cryogenic high-pressure gas jet cleaning technology can improve the wheel wear rate and debris morphology
[135]	Vegetable oil + water	–	AISI 52100	Wheel wear	Wheel cleaning technology can improve wheel wear
[136]	Vegetable oil	–	AISI 4340	Workpiece surface quality	1. Optimal MQL flow: 160 mL/h 2. High-pressure gas jet cleaning technology can further optimise the surface quality of the workpiece

and wheel cleanness was revealed. The unique grinding bottlenecks of the typical materials (titanium alloy, nickel-based alloy, and high-strength steel) were analysed. The physicochemical property and compatibility of the biolubricants under different grinding conditions were proposed. The specific conclusions are as follows:

(i) The long carbon chain, high fatty acid saturation and polar groups of biolubricants are the key characteristics to improve the adsorption capacity and strength of the lubricating oil film in the grinding zone. High viscosity and surface tension are beneficial to lubrication performance, whilst the cooling performance and wheel cleaning performance will be limited due to considerably high viscosity. Pour point, thermal stability, and pH value are the limiting conditions of the thermal/force boundary of the biolubricants, and the thermal stability of the grinding process should be emphatically considered.

(ii) The workpiece burn and material plastic accumulation of the titanium alloy was discovered in grinding due to its enhanced mechanical activity, low thermal conductivity and low elastic modulus. In comparison with the traditional cutting fluids, the normal force can be reduced by up to 72.2% with biolubricant. Meanwhile, the tangential force can be reduced by 79.1%, and the *Ra* value can be reduced by 52.07% using graphene + palm oil compared with pure oil. The advantage of biolubricant can be reflected by CoF and grinding temperature, which decreased from 0.562 to 0.384 °C and 278.90 to 229.18 °C, respectively. Moreover, the microhardness of the workpiece surface, the accumulation of the material plough and the adhesion of debris were significantly improved.

(iii) In the nickel-based alloy, the bottleneck of the wheel wear and workpiece surface burn was caused by its high hardness and low thermal conductivity. Palm oil as biolubricant has a better grinding performance than the

other types of vegetable oil. When Al₂O₃ + palm oil was used, the specific energy and friction coefficient were 31.2% and 38.3% lower than those of flood, respectively. The G-ratio increased from 0.688 to 1.532 due to the addition of Al₂O₃ nano-enhancer. Moreover, the use of biolubricants can significantly reduce the wheel wear, increase the G-ratio and control the surface defects caused by high grinding temperature.

(iv) In high-strength steel, the phenomenon of debris breaking difficulty, wheel blockage and high grinding temperature occur with the increase in tensile strength, which is directly reflected in the increase in microhardness and residual stress. In comparison with the cutting fluids, the tangential grinding force was reduced by 67.5% when using biolubricant, and the G-ratio was increased by 69.2% when utilising MWCNT + sunflower oil. Moreover, the residual stress and microhardness caused by high grinding temperature were significantly reduced when using nano-enhanced biolubricant.

(v) The physical and chemical characteristics of the biolubricants are also different due to the different grinding bottlenecks of difficult-to-machine materials. Titanium alloy grinding needs lubricants with strong lubrication and cooling capabilities and requires nano-enhancers with high thermal conductivity (e.g., graphene) and biolubricants with high viscosity (e.g., castor oil and palm oil). Nickel-based alloy grinding needs lubricants with modeling antiwear characteristics, and base oil should have high viscosity and fatty acid saturation, containing polar groups and other characteristics (e.g., palm oil and castor oil), nano-enhancers corresponding with high hardness and spherical characteristics (e.g., Al₂O₃). High-strength steel grinding needs lubricants with wheel cleaning performance, and low viscosity physical lubricants (e.g., canola oil and sunflower oil) are more suitable. The use of nano-enhancers can significantly improve the heat transfer performance, but there is no

need to make special requirements on their types and properties.

5 Future work and challenges

Figure 22 [89–92,96,107–119,121–124,127,128,130,132–140] is a summary of current research on vegetable oil. Although the substitution of biolubricants for traditional cutting fluids has been proven, some limitations remain [141–143]. The specific problems and future development trends are as follows:

(i) A large number of studies have been conducted on the molecular structure, viscosity and surface tension of biolubricants [144]. However, how the pH value and pour point change affect the lubrication performance of grinding and how to improve the grinding performance still lack of in-depth research. In the high temperature grinding zone, the biolubricant is easy to be oxidised at high temperature. How to improve the thermal stability is one of the difficult problems.

(ii) Biolubricants, especially vegetable oil, are widely produced in the world and used in industrial applications [145]. However, changes in the stability and oxidisability of biolubricant at high temperatures result in significant changes in their physicochemical and tribological properties; consequently, the oxidation properties of the biolubricant cannot meet the current needs of high pressure interface and heat dissipation [146]. In view of the

oxidation property at high temperature, the failure puzzle of biolubricant C=C can be solved by modifying it.

(iii) According to the problem of coordination between cooling and lubrication performance in the grinding of difficult-to-machine materials, the hybrid nano-enhancers and hybrid biolubricant methods were proposed and verified. However, the synergistic mechanism of the hybrid nano-enhancers, particle size ratio and concentration ratio on antiwear and heat dissipation need to be further analysed.

(iv) The excellent antifricition and antiwear performance of the nano-enhanced biolubricants is a guarantee to improve the surface quality of workpiece and improve tool wear. The adaptation between biolubricants and nano-enhancers (different types and concentrations) is the premise to ensure the excellent performance of nano-enhanced biolubricants [147]. Therefore, a case library for the compatibility of nano-enhanced biolubricants with different materials and processes must be created.

Nomenclature

Abbreviations

CBN	Cubic boron nitride
CNT	Carbon nano tube

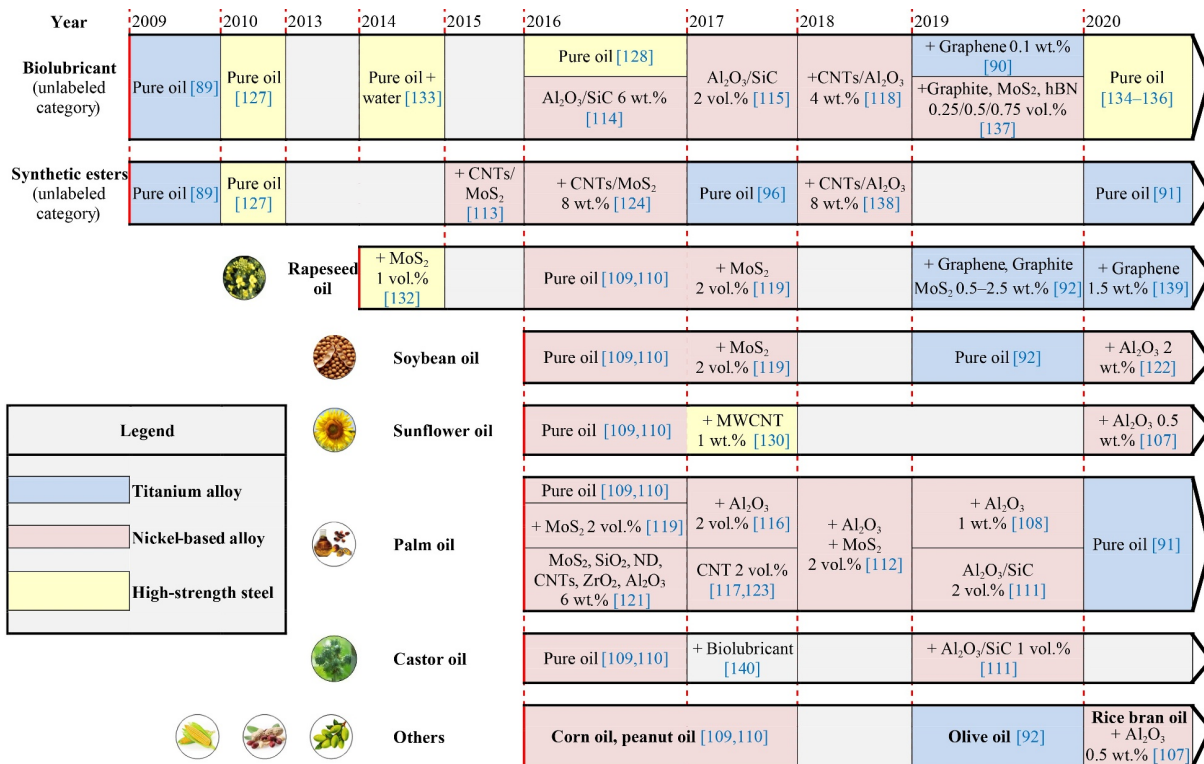


Fig. 22 Yearbook of grinding aerospace materials with biolubricants [89–92,96,107–119,121–124,127,128,130,132–140].

CoF	Coefficient of friction
CWCJ	Cooled wheel cleaning jet
EDS	Energy dispersive spectrometry
MQL	Minimum quantity lubrication
MWCNT	Multi-walled carbon nano tube
NMQL	Nanolubricant minimum quantity lubrication
SEM	Scanning electron microscopy
WCJ	Wheel cleaning jet

Variables

a_p	Grinding depth
F_n	Normal grinding force
F_t	Tangential grinding force
q_d	Heat flux density of debris
q_c	Heat flux density of the cooling medium
q_a	Heat flux density of abrasive
q_w	Heat flux density of the workpiece
Q_{total}	Total heat flux density
Ra	Surface roughness
V_s	Peripheral speed of grinding wheel
V_w	Workpiece feed speed
Λ_w	Material removal rate

Acknowledgements This research was financially supported by the National Natural Science Foundation of China (Grant Nos. 52105457 and 51975305), the National Key R&D Program of China (Grant No. 2020YFB2010500), the Shandong Natural Science Foundation, China (Grant Nos. ZR2020KE027 and ZR2020ME158), the Innovation Talent Supporting Program for Postdoctoral Fellows of Shandong Province, China (Grant No. SDBX2020012), and the Major Science and Technology Innovation Engineering Projects of Shandong Province, China (Grant No. 2019JZZY020111).

Open Access This article is licensed under a Creative Commons Attribution 4.0 International License, which permits use, sharing, adaptation, distribution, and reproduction in any medium or format as long as appropriate credit is given to the original author(s) and source, a link to the Creative Commons license is provided, and the changes made are indicated.

The images or other third-party material in this article are included in the article's Creative Commons license, unless indicated otherwise in a credit line to the material. If material is not included in the article's Creative Commons license and your intended use is not permitted by statutory regulation or exceeds the permitted use, you will need to obtain permission directly from the copyright holder.

Visit <http://creativecommons.org/licenses/by/4.0/> to view a copy of this license.

References

1. Najiha M S, Rahman M M, Yusoff A R. Environmental impacts and hazards associated with metal working fluids and recent advances in the sustainable systems: a review. *Renewable and*

2. Sustainable Energy Reviews, 2016, 60: 1008–1031
2. Ding W F, Zhu Y J, Xu J H, Fu Y C. Finite element investigation on the evolution of wear and stresses in brazed CBN grits during grinding. *The International Journal of Advanced Manufacturing Technology*, 2015, 81(5–8): 985–993
3. Wu X F, Li C H, Zhou Z M, Nie X L, Chen Y, Zhang Y B, Cao H J, Liu B, Zhang N Q, Said Z, Debnath S, Jamil M, Ali H M, Sharma S. Circulating purification of cutting fluid: an overview. *The International Journal of Advanced Manufacturing Technology*, 2021, 117(9–10): 2565–2600
4. Jia D Z, Li C H, Wang S, Zhang Q. Investigation into distributing characteristic of suspend particulate in MQL grinding. *Manufacturing Technology and Machine Tool*, 2014, (2): 58–61 (in Chinese)
5. Shokrani A, Dhokia V, Newman S T. Environmentally conscious machining of difficult-to-machine materials with regard to cutting fluids. *International Journal of Machine Tools and Manufacture*, 2012, 57: 83–101
6. Liu M Z, Li C H, Cao H J, Zhang S, Chen Y, Liu B, Zhang N Q, Zhou Z M. Research progress and application of CMQL machining technology. *China Mechanical Engineering*, 2022, 33(5): 529–550 (in Chinese)
7. Pusavec F, Kramar D, Krajnik P, Kopac J. Transitioning to sustainable production—part II: evaluation of sustainable machining technologies. *Journal of Cleaner Production*, 2010, 18(12): 1211–1221
8. Sanchez J A, Pombo I, Alberdi R, Izquierdo B, Ortega N, Plaza S, Martinez-Toledano J. Machining evaluation of a hybrid MQL-CO₂ grinding technology. *Journal of Cleaner Production*, 2010, 18(18): 1840–1849
9. Li H G, Zhang Y B, Li C H, Zhou Z M, Nie X L, Chen Y, Cao H J, Liu B, Zhang N Q, Said Z, Debnath S, Jamil M, Ali H M, Sharma S. Cutting fluid corrosion inhibitors from inorganic to organic: progress and applications. *Korean Journal of Chemical Engineering*, 2022, 39(5): 1107–1134
10. Jia D Z, Li C H, Zhang Y B, Yang M, Zhang X P, Li R Z, Ji H J. Experimental evaluation of surface topographies of NMQL grinding ZrO₂ ceramics combining multiangle ultrasonic vibration. *The International Journal of Advanced Manufacturing Technology*, 2019, 100(1–4): 457–473
11. Jia D Z, Li C H, Wang S, Zhang Q, Hou Y L. Advances and patents about grinding equipments with nano-particle jet minimum quantity lubrication. *Recent Patents on Nanotechnology*, 2014, 8(3): 215–229
12. Wang C Y, Xie Y X, Qin Z, Lin H S, Yuan Y H, Wang Q M. Wear and breakage of TiAlN- and TiSiN-coated carbide tools during high-speed milling of hardened steel. *Wear*, 2015, 336–337: 29–42
13. Wang W, Yao P, Wang J, Huang C Z, Zhu H T, Zou B, Liu H L, Yan J W. Crack-free ductile mode grinding of fused silica under controllable dry grinding conditions. *International Journal of Machine Tools and Manufacture*, 2016, 109: 126–136
14. Agarwal S, Venkateswara Rao P. Performance improvement of SiC grinding using solid lubricants. *Machining Science and Technology*, 2007, 11(1): 61–79
15. Park K H, Suhaimi M A, Yang G D, Lee D Y, Lee S W, Kwon P.

- Milling of titanium alloy with cryogenic cooling and minimum quantity lubrication (MQL). *International Journal of Precision Engineering and Manufacturing*, 2017, 18(1): 5–14
16. Zhang J C, Li C H, Zhang Y B, Yang M, Jia D Z, Liu G T, Hou Y L, Li R Z, Zhang N Q, Wu Q D, Cao H J. Experimental assessment of an environmentally friendly grinding process using nanofluid minimum quantity lubrication with cryogenic air. *Journal of Cleaner Production*, 2018, 193: 236–248
 17. Tawakoli T, Hadad M, Sadeghi M H, Daneshi A, Sadeghi B. Minimum quantity lubrication in grinding: effects of abrasive and coolant–lubricant types. *Journal of Cleaner Production*, 2011, 19(17–18): 2088–2099
 18. Barczak L M, Batako A D L, Morgan M N. A study of plane surface grinding under minimum quantity lubrication (MQL) conditions. *International Journal of Machine Tools and Manufacture*, 2010, 50(11): 977–985
 19. Tawakoli T, Hadad M, Sadeghi M H, Daneshi A, Stöckert S, Rasifard A. An experimental investigation of the effects of workpiece and grinding parameters on minimum quantity lubrication—MQL grinding. *International Journal of Machine Tools and Manufacture*, 2009, 49(12–13): 924–932
 20. Ejaz A, Babar H, Ali H M, Jamil F, Janjua M M, Fattah I M R, Said Z, Li C H. Concentrated photovoltaics as light harvesters: outlook, recent progress, and challenges. *Sustainable Energy Technologies and Assessments*, 2021, 46: 101199
 21. Liu M Z, Li C H, Zhang Y B, An Q L, Yang M, Gao T, Mao C, Liu B, Cao H J, Xu X F, Said Z, Debnath S, Jamil M, Ali H M, Sharma S. Cryogenic minimum quantity lubrication machining: from mechanism to application. *Frontiers of Mechanical Engineering*, 2021, 16(4): 649–697
 22. Zhang Y B, Li C H, Ji H J, Yang X H, Yang M, Jia D Z, Zhang X P, Li R Z, Wang J. Analysis of grinding mechanics and improved predictive force model based on material-removal and plastic-stacking mechanisms. *International Journal of Machine Tools and Manufacture*, 2017, 122: 81–97
 23. Huang S Q, Wu H, Jiang Z Y, Huang H. Water-based nanosuspensions: formulation, tribological property, lubrication mechanism, and applications. *Journal of Manufacturing Processes*, 2021, 71: 625–644
 24. Zainal N A, Zulkifli N W M, Gulzar M, Masjuki H H. A review on the chemistry, production, and technological potential of bio-based lubricants. *Renewable and Sustainable Energy Reviews*, 2018, 82(1): 80–102
 25. Yang M, Li C H, Zhang Y B, Wang Y G, Li B K, Jia D Z, Hou Y L, Li R Z. Research on microscale skull grinding temperature field under different cooling conditions. *Applied Thermal Engineering*, 2017, 126(1): 525–537
 26. Jia D Z, Zhang Y B, Li C H, Yang M, Gao T, Said Z, Sharma S. Lubrication-enhanced mechanisms of titanium alloy grinding using lecithin biolubricant. *Tribology International*, 2022, 169: 107461
 27. Yang M, Li C H, Luo L, Li R Z, Long Y Z. Predictive model of convective heat transfer coefficient in bone micro-grinding using nanofluid aerosol cooling. *International Communications in Heat and Mass Transfer*, 2021, 125: 105317
 28. Gao T, Li C H, Yang M, Zhang Y B, Jia D Z, Ding W F, Debnath S, Yu T B, Said Z, Wang J. Mechanics analysis and predictive force models for the single-diamond grain grinding of carbon fiber reinforced polymers using CNT nano-lubricant. *Journal of Materials Processing Technology*, 2021, 290(9–12): 116976
 29. Klocke F, Soo S L, Karpuschewski B, Webster J A, Novovic D, Elfizy A, Axinte D A, Tönissena S. Abrasive machining of advanced aerospace alloys and composites. *CIRP Annals*, 2015, 64(2): 581–604
 30. Li S, Wu Y, Yamamura K, Nomura M, Fujii T. Improving the grindability of titanium alloy Ti–6Al–4V with the assistance of ultrasonic vibration and plasma electrolytic oxidation. *CIRP Annals*, 2017, 66(1): 345–348
 31. Zhu S W, Xiao G J, He Y, Liu G, Song S Y, Jiahua S L. Tip vortex cavitation of propeller bionic noise reduction surface based on precision abrasive belt grinding. *Journal of Advanced Manufacturing Science and Technology*, 2022, 2(1): 2022003
 32. Sinha M K, Setti D, Ghosh S, Venkateswara Rao P. An investigation on surface burn during grinding of Inconel 718. *Journal of Manufacturing Processes*, 2016, 21: 124–133
 33. Nadolny K, Rokosz K, Kaplonek W, Wienecke M, Heeg J. SEM-EDS-based analysis of the amorphous carbon-treated grinding wheel active surface after reciprocal internal cylindrical grinding of Titanium Grade 2[®] alloy. *The International Journal of Advanced Manufacturing Technology*, 2017, 90(5–8): 2293–2308
 34. Qu S S, Yao P, Gong Y D, Yang Y Y, Chu D K. Modelling and grinding characteristics of unidirectional C–SiCs. *Ceramics International*, 2022, 48(6): 8314–8324
 35. Ulutan D, Ozel T. Machining induced surface integrity in titanium and nickel alloys: a review. *International Journal of Machine Tools and Manufacture*, 2011, 51(3): 250–280
 36. Ezugwu E O. Key improvements in the machining of difficult-to-cut aerospace superalloys. *International Journal of Machine Tools and Manufacture*, 2005, 45(12–13): 1353–1367
 37. Hu D Y, Wang X Y, Mao J X, Wang R Q. Creep-fatigue crack growth behavior in GH4169 superalloy. *Frontiers of Mechanical Engineering*, 2019, 14(3): 369–376
 38. Ye H T, Zhang J, Yang J F, Liu Y. Key application technology of cutting for aircraft difficult-to-machine material. *Aeronautical Manufacturing Technology*, 2012, 406(10): 44–46 (in Chinese)
 39. Wang Y, Wang W L. Advanced cutting tool technology for aircraft component machining. *Aeronautical Manufacturing Technology*, 2009, (23): 36–42 (in Chinese)
 40. Gao T, Zhang Y B, Li C H, Wang Y Q, An Q L, Liu B, Said Z, Sharma S. Grindability of carbon fiber reinforced polymer using CNT biological lubricant. *Scientific Reports*, 2021, 11(1): 22535
 41. Duan Z J, Li C H, Ding W F, Zhang Y B, Yang M, Gao T, Cao H J, Xu X F, Wang D Z, Mao C, Li H N, Kumar G M, Said Z, Debnath S, Jamil M, Ali H M. Milling force model for aviation aluminum alloy: academic insight and perspective analysis. *Chinese Journal of Mechanical Engineering*, 2021, 34(1): 18
 42. Yang Y Y, Gong Y D, Li C H, Wen X L, Sun J Y. Mechanical performance of 316 L stainless steel by hybrid directed energy deposition and thermal milling process. *Journal of Materials Processing Technology*, 2021, 291: 117023
 43. Ding W F, Xu J H, Chen Z Z, Su H H, Fu Y C. Grain wear of brazed polycrystalline CBN abrasive tools during constant-force

- grinding Ti-6Al-4V alloy. *The International Journal of Advanced Manufacturing Technology*, 2011, 52(9-12): 969-976
44. Mao C, Lu J, Zhao Z H, Yin L R, Hu Y L, Bi Z M. Simulation and experiment of cutting characteristics for single cBN-WC-10Co fiber. *Precision Engineering*, 2018, 52: 170-182
 45. Gao T, Li C H, Wang Y Q, Liu X S, An Q L, Li H N, Zhang Y B, Cao H J, Liu B, Wang D Z, Said Z, Debnath S, Jamil M, Ali H M, Sharma S. Carbon fiber reinforced polymer in drilling: from damage mechanisms to suppression. *Composite Structures*, 2022, 286: 115232
 46. Xi X X, Yu T Y, Ding W F, Xu J H. Grinding of Ti₂AlNb intermetallics using silicon carbide and alumina abrasive wheels: tool surface topology effect on grinding force and ground surface quality. *Precision Engineering*, 2018, 53: 134-145
 47. Thakur A, Gangopadhyay S. State-of-the-art in surface integrity in machining of nickel-based super alloys. *International Journal of Machine Tools and Manufacture*, 2016, 100: 25-54
 48. Sun Y, Jin L Y, Gong Y D, Wen X L, Yin G Q, Wen Q, Tang B J. Experimental evaluation of surface generation and force time-varying characteristics of curvilinear grooved micro end mills fabricated by EDM. *Journal of Manufacturing Processes*, 2022, 73: 799-814
 49. Cui X, Li C H, Ding W F, Chen Y, Mao C, Xu X F, Liu B, Wang D Z, Li H N, Zhang Y B, Said Z, Debnath S, Jamil M, Ali H M, Sharma S. Minimum quantity lubrication machining of aeronautical materials using carbon group nanolubricant: from mechanisms to application. *Chinese Journal of Aeronautics*, 2022, 35(11): 85-112
 50. Wang X M, Li C H, Zhang Y B, Said Z, Debnath S, Sharma S, Yang M, Gao T. Influence of texture shape and arrangement on nanofluid minimum quantity lubrication turning. *The International Journal of Advanced Manufacturing Technology*, 2022, 119(1-2): 631-646
 51. Jia D Z, Li C H, Zhang D K, Zhang Y B, Zhang X W. Experimental verification of nanoparticle jet minimum quantity lubrication effectiveness in grinding. *Journal of Nanoparticle Research*, 2014, 16(12): 2758
 52. Cui X, Li C H, Zhang Y B, Jia D Z, Zhao Y J, Li R Z, Cao H J. Tribological properties under the grinding wheel and workpiece interface by using graphene nanofluid lubricant. *The International Journal of Advanced Manufacturing Technology*, 2019, 104(9-12): 3943-3958
 53. Tang L Z, Zhang Y B, Li C H, Zhou Z M, Nie X L, Chen Y, Cao H J, Liu B, Zhang N Q, Said Z, Debnath S, Jamil M, Ali H M, Sharma S. Biological stability of water-based cutting fluids: progress and application. *Chinese Journal of Mechanical Engineering*, 2022, 35(1): 3
 54. Gupta M K, Khan A M, Song Q H, Liu Z Q, Khalid Q S, Jamil M, Kuntoğlu M, Usca Ü A, Sarikaya M, Pimenov D Y. A review on conventional and advanced minimum quantity lubrication approaches on performance measures of grinding process. *The International Journal of Advanced Manufacturing Technology*, 2021, 117(3-4): 729-750
 55. Pimenov D Y, Mia M, Gupta M K, Machado A R, Tomaz Í V, Sarikaya M, Wojciechowski S, Mikolajczyk T, Kaplonek W. Improvement of machinability of Ti and its alloys using cooling-lubrication techniques: a review and future prospect. *Journal of Materials Research and Technology*, 2021, 11: 719-753
 56. Singh A K, Kumar A, Sharma V, Kala P. Sustainable techniques in grinding: state of the art review. *Journal of Cleaner Production*, 2020, 269: 121876
 57. Said Z, Gupta M, Hegab H, Arora N, Khan A M, Jamil M, Bellos E. A comprehensive review on minimum quantity lubrication (MQL) in machining processes using nano-cutting fluids. *The International Journal of Advanced Manufacturing Technology*, 2019, 105(5-6): 2057-2086
 58. Awale A S, Srivastava A, Vashista M, Khan Yusufzai M Z. Influence of minimum quantity lubrication on surface integrity of ground hardened H13 hot die steel. *The International Journal of Advanced Manufacturing Technology*, 2019, 100(1-4): 983-997
 59. Hosseini S F, Emami M, Sadeghi M H. An experimental investigation on the effects of minimum quantity nano lubricant application in grinding process of tungsten carbide. *Journal of Manufacturing Processes*, 2018, 35: 244-253
 60. Hadad M, Hadi M. An investigation on surface grinding of hardened stainless steel S34700 and aluminum alloy AA6061 using minimum quantity of lubrication (MQL) technique. *The International Journal of Advanced Manufacturing Technology*, 2013, 68(9-12): 2145-2158
 61. Emami M, Sadeghi M H, Sarhan A A D, Hasani F. Investigating the minimum quantity lubrication in grinding of Al₂O₃ engineering ceramic. *Journal of Cleaner Production*, 2014, 66: 632-643
 62. Kelly J F, Cotterell M G. Minimal lubrication machining of aluminium alloys. *Journal of Materials Processing Technology*, 2002, 120(1-3): 327-334
 63. Zhang Y B, Li H N, Li C H, Huang C Z, Ali H M, Xu X F, Mao C, Ding W F, Cui X, Yang M, Yu T B, Jamil M, Gupta M K, Jia D Z, Said Z. Nano-enhanced biolubricant in sustainable manufacturing: from processability to mechanisms. *Friction*, 2022, 10(6): 803-841
 64. Wang X M, Li C H, Zhang Y B, Ding W F, Yang M, Gao T, Cao H J, Xu X F, Wang D Z, Said Z, Debnath S, Jamil M, Ali H M. Vegetable oil-based nanofluid minimum quantity lubrication turning: academic review and perspectives. *Journal of Manufacturing Processes*, 2020, 59: 76-97
 65. Hou B, Chen B S, Fang J H, Huang W J. Application of vegetable oil in biodegradable lubricants. *Synthetic Lubricants*, 2002, 29(3): 21-25 (in Chinese)
 66. Shi Z, Guo S M, Liu H J, Li C H, Zhang Y B, Yang M, Chen Y, Liu B, Zhou Z M, Nie X L. Experimental evaluation of minimum quantity lubrication of biological lubricant on grinding properties of GH4169 nickel-base alloy. *Surface Technology*, 2021, 50(12): 71-84 (in Chinese)
 67. Bai X F, Li C H, Dong L, Yin Q A. Experimental evaluation of the lubrication performances of different nanofluids for minimum quantity lubrication (MQL) in milling Ti-6Al-4V. *The International Journal of Advanced Manufacturing Technology*, 2019, 101(9-12): 2621-2632
 68. Yang M, Li C H, Said Z, Zhang Y B, Li R Z, Debnath S, Ali H M, Gao T, Long Y Z. Semiempirical heat flux model of hard-brittle bone material in ductile microgrinding. *Journal of*

- Manufacturing Processes, 2021, 71: 501–514
69. Zhang J C, Wu W T, Li C H, Yang M, Zhang Y B, Jia D Z, Hou Y L, Li R Z, Cao H J, Ali H M. Convective heat transfer coefficient model under nanofluid minimum quantity lubrication coupled with cryogenic air grinding Ti–6Al–4V. *International Journal of Precision Engineering and Manufacturing-Green Technology*, 2021, 8(4): 1113–1135
 70. Yang M, Li C H, Zhang Y B, Jia D Z, Zhang X P, Hou Y L, Li R Z, Wang J. Maximum undeformed equivalent chip thickness for ductile-brittle transition of zirconia ceramics under different lubrication conditions. *International Journal of Machine Tools and Manufacture*, 2017, 122: 55–65
 71. Yang M, Li C H, Zhang Y B, Jia D Z, Li R Z, Hou Y L, Cao H J, Wang J. Predictive model for minimum chip thickness and size effect in single diamond grain grinding of zirconia ceramics under different lubricating conditions. *Ceramics International*, 2019, 45(12): 14908–14920
 72. Wang Y G, Li C H, Zhang Y B, Li B K, Yang M, Zhang X P, Guo S M, Liu G T, Zhai M G. Comparative evaluation of the lubricating properties of vegetable-oil-based nanofluids between frictional test and grinding experiment. *Journal of Manufacturing Processes*, 2017, 26: 94–104
 73. Zhao Y J, Xu W H, Xi C Z, Liang D T, Li H N. Automatic and accurate measurement of microhardness profile based on image processing. *IEEE Transactions on Instrumentation and Measurement*, 2021, 70: 1–9
 74. Gao T, Li C H, Jia D Z, Zhang Y B, Yang M, Wang X M, Cao H J, Li R Z, Ali H M, Xu X F. Surface morphology assessment of CFRP transverse grinding using CNT nanofluid minimum quantity lubrication. *Journal of Cleaner Production*, 2020, 277: 123328
 75. Jia D Z, Zhang N Q, Liu B, Zhou Z M, Wang X P, Zhang Y B, Mao C, Li C H. Particle size distribution characteristics of electrostatic minimum quantity lubrication and grinding surface quality evaluation. *Diamond and Abrasives Engineering*, 2021, 41(3): 89–95 (in Chinese)
 76. Debnath S, Reddy M M, Yi Q S. Environmental friendly cutting fluids and cooling techniques in machining: a review. *Journal of Cleaner Production*, 2014, 83: 33–47
 77. Yin Q A, Li C H, Dong L, Bai X F, Zhang Y B, Yang M, Jia D Z, Li R Z, Liu Z Q. Effects of physicochemical properties of different base oils on friction coefficient and surface roughness in MQL milling AISI 1045. *International Journal of Precision Engineering and Manufacturing-Green Technology*, 2021, 8(6): 1629–1647
 78. Zhang Y B, Li C H, Jia D Z, Zhang D K, Zhang X W. Experimental evaluation of MoS₂ nanoparticles in jet MQL grinding with different types of vegetable oil as base oil. *Journal of Cleaner Production*, 2015, 87: 930–940
 79. Chawaloeshonsiya N, Guiraud P, Painmanakul P. Analysis of cutting-oil emulsion destabilization by aluminum sulfate. *Environmental Technology*, 2018, 39(11): 1450–1460
 80. Tao D H, Li Q H. CN Patent, 200910053886, 2010-08-04 (in Chinese)
 81. Zhang X, Ma X T, Zhang W, Wu J Q, Yu S S, Nie K L, Chen B Q, Tan T W. CN Patent, 201911009773, 2020-04-28 (in Chinese)
 82. Wang Z G, Shen Q. CN Patent, 201510725351, 2016-02-03 (in Chinese)
 83. Wang X, Ding W F, Zhao B. A review on machining technology of aero-engine casings. *Journal of Advanced Manufacturing Science and Technology*, 2022, 2(3): 2022011
 84. Wang D, Cao H R. A comprehensive review on crack modeling and detection methods of aero-engine disks. *Journal of Advanced Manufacturing Science and Technology*, 2022, 2(3): 2022012
 85. Ding W F, Xi X X, Zhan J H, Xu J H, Fu Y C, Su H H. Research status and future development of grinding technology of titanium materials for aero-engines. *Acta Aeronautica et Astronautica Sinica*, 2019, 40(6): 022763 (in Chinese)
 86. Xiao G J, Zhang Y D, Huang Y, Song S Y, Chen B Q. Grinding mechanism of titanium alloy: research status and prospect. *Journal of Advanced Manufacturing Science and Technology*, 2021, 1(1): 2020001
 87. Sun T, Qin L F, Hou J M, Fu Y C. Machinability of damage-tolerant titanium alloy in orthogonal turn-milling. *Frontiers of Mechanical Engineering*, 2020, 15(3): 504–515
 88. Krishnan A, Fang F Z. Review on mechanism and process of surface polishing using lasers. *Frontiers of Mechanical Engineering*, 2019, 14(3): 299–319
 89. Sadeghi M H, Haddad M J, Tawakoli T, Emami M. Minimal quantity lubrication-MQL in grinding of Ti–6Al–4V titanium alloy. *The International Journal of Advanced Manufacturing Technology*, 2009, 44(5–6): 487–500
 90. Li M, Yu T B, Zhang R C, Yang L, Ma Z L, Li B C, Wang X Z, Wang W S, Zhao J. Experimental evaluation of an eco-friendly grinding process combining minimum quantity lubrication and graphene-enhanced plant-oil-based cutting fluid. *Journal of Cleaner Production*, 2020, 244: 118747
 91. Ibrahim A M M, Li W, Xiao H, Zeng Z X, Ren Y H, Alsoufi M S. Energy conservation and environmental sustainability during grinding operation of Ti–6Al–4V alloys via eco-friendly oil/graphene nano additive and minimum quantity lubrication. *Tribology International*, 2020, 150: 106387
 92. Singh H, Sharma V S, Singh S, Dogra M. Nanofluids assisted environmental friendly lubricating strategies for the surface grinding of titanium alloy: Ti–6Al–4V-ELI. *Journal of Manufacturing Processes*, 2019, 39: 241–249
 93. Setti D, Sinha M K, Ghosh S, Venkateswara Rao P. Performance evaluation of Ti–6Al–4V grinding using chip formation and coefficient of friction under the influence of nanofluids. *International Journal of Machine Tools and Manufacture*, 2015, 88: 237–248
 94. Wang X M, Zhang J C, Wang X P, Zhang Y B, Liu B, Luo L, Zhao W, Zhang N Q, Nie X L, Li C H. Effect of nanoparticle volume on grinding performance of titanium alloy in cryogenic air minimum quantity lubrication. *Diamond and Abrasives Engineering*, 2020, 40(5): 23–29 (in Chinese)
 95. Huang B T, Li C H, Zhang Y B, Ding W F, Yang M, Yang Y Y, Zhai H, Xu X F, Wang D Z, Debnath S, Jamil M, Li H N, Ali H M, Gupta M K, Said Z. Advances in fabrication of ceramic corundum abrasives based on sol–gel process. *Chinese Journal of Aeronautics*, 2021, 34(6): 1–17
 96. Liu G T, Li C H, Zhang Y B, Yang M, Jia D Z, Zhang X P, Guo

- S M, Li R Z, Zhai H. Process parameter optimization and experimental evaluation for nanofluid MQL in grinding Ti-6Al-4V based on grey relational analysis. *Materials and Manufacturing Processes*, 2018, 33(9): 950–963
97. Li C H, Li J Y, Wang S, Zhang Q. Modeling and numerical simulation of the grinding temperature field with nanoparticle jet of MQL. *Advances in Mechanical Engineering*, 2013, 5: 986984
 98. Yang M, Li C H, Zhang Y B, Jia D Z, Zhang X P, Li R Z. A new model for predicting neurosurgery skull bone grinding temperature field. *Journal of Mechanical Engineering*, 2018, 54(23): 215–222 (in Chinese)
 99. Yang M, Li C H, Luo L, Li R Z, Long Y Z. Predictive model of convective heat transfer coefficient in bone micro-grinding using nanofluid aerosol cooling. *International Communications in Heat and Mass Transfer*, 2021, 125: 105317
 100. Wang X M, Zhang J C, Wang X P, Zhang Y B, Luo L, Zhao W, Liu B, Nie X L, Li C H. Temperature field model and verification of titanium alloy grinding under different cooling conditions. *China Mechanical Engineering*, 2021, 32(5): 572–578, 586 (in Chinese)
 101. Yang M, Li C H, Zhang Y B, Wang Y G, Li B K, Li R Z. Theoretical analysis and experimental research on temperature field of microscale bone grinding under nanoparticle jet mist cooling. *Journal of Mechanical Engineering*, 2018, 54(18): 194–203 (in Chinese)
 102. Cui X, Li C H, Zhang Y B, Said Z, Debnath S, Sharma S, Ali H M, Yang M, Gao T, Li R Z. Grindability of titanium alloy using cryogenic nanolubricant minimum quantity lubrication. *Journal of Manufacturing Processes*, 2022, 80: 273–286
 103. Li C H, Yang M, Zhang Y B, Zhang N Q, Liu B. Design of Case Base for Intelligent and Clean Precision Manufacturing of MQL. Beijing: Science Press, 2020 (in Chinese)
 104. M'Saoubi R, Axinte D, Soo S L, Nobel C, Attia H, Kappmeyer G, Engin S, Sim W M. High performance cutting of advanced aerospace alloys and composite materials. *CIRP Annals*, 2015, 64(2): 557–580
 105. Akhtar W, Sun J F, Sun P F, Chen W Y, Saleem Z. Tool wear mechanisms in the machining of Nickel based super-alloys: a review. *Frontiers of Mechanical Engineering*, 2014, 9(2): 106–119
 106. Wang X Y, Huang C Z, Zou B, Liu G L, Zhu H T, Wang J. Experimental study of surface integrity and fatigue life in the face milling of Inconel 718. *Frontiers of Mechanical Engineering*, 2018, 13(2): 243–250
 107. Viridi R L, Chatha S S, Singh H. Machining performance of Inconel-718 alloy under the influence of nanoparticles based minimum quantity lubrication grinding. *Journal of Manufacturing Processes*, 2020, 59: 355–365
 108. Viridi R L, Chatha S S, Singh H. Experiment evaluation of grinding properties under Al₂O₃ nanofluids in minimum quantity lubrication. *Materials Research Express*, 2019, 6(9): 096574
 109. Wang Y G, Li C H, Zhang Y B, Yang M, Li B K, Jia D Z, Hou Y L, Mao C. Experimental evaluation of the lubrication properties of the wheel/workpiece interface in minimum quantity lubrication (MQL) grinding using different types of vegetable oils. *Journal of Cleaner Production*, 2016, 127: 487–499
 110. Li B K, Li C H, Zhang Y B, Wang Y G, Jia D Z, Yang M. Grinding temperature and energy ratio coefficient in MQL grinding of high-temperature nickel-base alloy by using different vegetable oils as base oil. *Chinese Journal of Aeronautics*, 2016, 29(4): 1084–1095
 111. Zhang X P, Li C H, Jia D Z, Gao T, Zhang Y B, Yang M, Li R Z, Han Z G, Ji H J. Spraying parameter optimization and microtopography evaluation in nanofluid minimum quantity lubrication grinding. *The International Journal of Advanced Manufacturing Technology*, 2019, 103(5–8): 2523–2539
 112. Wang Y G, Li C H, Zhang Y B, Yang M, Li B K, Dong L, Wang J. Processing characteristics of vegetable oil-based nanofluid MQL for grinding different workpiece materials. *International Journal of Precision Engineering and Manufacturing-Green Technology*, 2018, 5(2): 327–339
 113. Zhang Y B, Li C H, Jia D Z, Zhang D K, Zhang X W. Experimental evaluation of the lubrication performance of MoS₂/CNT nanofluid for minimal quantity lubrication in Ni-based alloy grinding. *International Journal of Machine Tools and Manufacture*, 2015, 99: 19–33
 114. Zhang X P, Li C H, Zhang Y B, Jia D Z, Li B K, Wang Y G, Yang M, Hou Y L, Zhang X W. Performances of Al₂O₃/SiC hybrid nanofluids in minimum-quantity lubrication grinding. *The International Journal of Advanced Manufacturing Technology*, 2016, 86(9–12): 3427–3441
 115. Zhang X P, Li C H, Zhang Y B, Wang Y G, Li B K, Yang M, Guo S M, Liu G T, Zhang N Q. Lubricating property of MQL grinding of Al₂O₃/SiC mixed nanofluid with different particle sizes and microtopography analysis by cross-correlation. *Precision Engineering*, 2017, 47: 532–545
 116. Wang Y G, Li C H, Zhang Y B, Yang M, Zhang X P, Zhang N Q, Dai J J. Experimental evaluation on tribological performance of the wheel/workpiece interface in minimum quantity lubrication grinding with different concentrations of Al₂O₃ nanofluids. *Journal of Cleaner Production*, 2017, 142: 3571–3583
 117. Li B K, Li C H, Zhang Y B, Wang Y G, Yang M, Jia D Z, Zhang N Q, Wu Q D. Effect of the physical properties of different vegetable oil-based nanofluids on MQLC grinding temperature of Ni-based alloy. *The International Journal of Advanced Manufacturing Technology*, 2017, 89(9–12): 3459–3474
 118. Hegab H, Darras B, Kishawy H A. Sustainability assessment of machining with nano-cutting fluids. *Procedia Manufacturing*, 2018, 26: 245–254
 119. Zhang Y B, Li C H, Yang M, Jia D Z, Wang Y G, Li B K, Hou Y L, Zhang N Q, Wu Q D. Experimental evaluation of cooling performance by friction coefficient and specific friction energy in nanofluid minimum quantity lubrication grinding with different types of vegetable oil. *Journal of Cleaner Production*, 2016, 139: 685–705
 120. Li B K, Li C H, Zhang Y B, Wang Y G, Jia D Z, Yang M, Zhang N Q, Wu Q D, Han Z G, Sun K. Heat transfer performance of MQL grinding with different nanofluids for Ni-based alloys using vegetable oil. *Journal of Cleaner Production*, 2017, 154: 1–11
 121. Wang Y G, Li C H, Zhang Y B, Li B K, Yang M, Zhang X P, Guo S M, Liu G T. Experimental evaluation of the lubrication properties of the wheel/workpiece interface in MQL grinding

- with different nanofluids. *Tribology International*, 2016, 99: 198–210
122. Peng R T, He X B, Tong J W, Tang X Z, Wu Y P. Application of a tailored eco-friendly nanofluid in pressurized internal-cooling grinding of Inconel 718. *Journal of Cleaner Production*, 2021, 278: 123498
 123. Li B K, Li C H, Zhang Y B, Wang Y G, Yang M, Jia D Z, Zhang N Q, Wu Q D, Ding W F. Numerical and experimental research on the grinding temperature of minimum quantity lubrication cooling of different workpiece materials using vegetable oil-based nanofluids. *The International Journal of Advanced Manufacturing Technology*, 2017, 93(5–8): 1971–1988
 124. Zhang Y B, Li C H, Jia D Z, Li B K, Wang Y G, Yang M, Hou Y L, Zhang X W. Experimental study on the effect of nanoparticle concentration on the lubricating property of nanofluids for MQL grinding of Ni-based alloy. *Journal of Materials Processing Technology*, 2016, 232: 100–115
 125. Zhang Z C, Sui M H, Li C H, Zhou Z M, Liu B, Chen Y, Said Z, Debnath S, Sharma S. Residual stress of grinding cemented carbide using MoS₂ nano-lubricant. *The International Journal of Advanced Manufacturing Technology*, 2022, 119(9–10): 5671–5685
 126. Sui M H, Li C H, Wu W T, Yang M, Ali H M, Zhang Y B, Jia D Z, Hou Y L, Li R Z, Cao H J. Temperature of grinding carbide with castor oil-based MoS₂ nanofluid minimum quantity lubrication. *Journal of Thermal Science and Engineering Applications*, 2021, 13(5): 1–30
 127. Sadeghi M H, Hadad M J, Tawakoli T, Vesali A, Emami M. An investigation on surface grinding of AISI 4140 hardened steel using minimum quantity lubrication-MQL technique. *International Journal of Material Forming*, 2010, 3(4): 241–251
 128. Shao Y M, Fergani O, Ding Z S, Li B Z, Liang S Y. Experimental investigation of residual stress in minimum quantity lubrication grinding of AISI 1018 steel. *Journal of Manufacturing Science and Engineering*, 2016, 138(1): 011009
 129. Mao C, Tang X J, Zou H F, Huang X M, Zhou Z X. Investigation of grinding characteristic using nanofluid minimum quantity lubrication. *International Journal of Precision Engineering and Manufacturing*, 2012, 13(10): 1745–1752
 130. ManojKumar K, Ghosh A. Assessment of cooling-lubrication and wettability characteristics of nano-engineered sunflower oil as cutting fluid and its impact on SQCL grinding performance. *Journal of Materials Processing Technology*, 2016, 237: 55–64
 131. Molaie M M, Zahedi A, Akbari J. Effect of water-based nanolubricants in ultrasonic vibration assisted grinding. *Journal of Manufacturing and Materials Processing*, 2018, 2(4): 80
 132. Mao C, Zhang J, Huang Y, Zou H F, Huang X M, Zhou Z X. Investigation on the effect of nanofluid parameters on MQL grinding. *Materials and Manufacturing Processes*, 2013, 28(4): 436–442
 133. de Mello Belentani R, Júnior H F, Canarim R C, Diniz A E, Hassui A, Aguiar P R, Bianchi E C. Utilization of minimum quantity lubrication (MQL) with water in CBN grinding of steel. *Materials Research*, 2014, 17(1): 88–96
 134. Javaroni R L, Lopes J C, Diniz A E, Garcia M V, Ribeiro F S F, Tavares A B, Talon A G, Sanchez L E d A, de Mello H J, Aguiar P R, Bianchi E C. Improvement in the grinding process using the MQL technique with cooled wheel cleaning jet. *Tribology International*, 2020, 152: 106512
 135. Garcia M V, Lopes J C, Diniz A E, Rodrigues A R, Volpato R S, de Angelo Sanchez L E, de Mello H J, Aguiar P R, Bianchi E C. Grinding performance of bearing steel using MQL under different dilutions and wheel cleaning for green manufacture. *Journal of Cleaner Production*, 2020, 257: 120376
 136. Javaroni R L, Lopes J C, Garcia M V, Ribeiro F S F, de Angelo Sanchez L E, de Mello H J, Aguiar P R, Bianchi E C. Grinding hardened steel using MQL associated with cleaning system and cBN wheel. *The International Journal of Advanced Manufacturing Technology*, 2020, 107(5–6): 2065–2080
 137. Şirin Ş, Kıvak T. Performances of different eco-friendly nanofluid lubricants in the milling of Inconel X-750 superalloy. *Tribology International*, 2019, 137: 180–192
 138. Zhang Y B, Li C H, Jia D Z, Li B K, Wang Y G, Yang M, Hou Y L, Zhang N Q, Wu Q D. Experimental evaluation of the workpiece surface quality of MoS₂/CNT nanofluid for minimal quantity lubrication in grinding. *Journal of Mechanical Engineering*, 2018, 54(1): 161–170 (in Chinese)
 139. Singh H, Sharma V S, Dogra M. Exploration of graphene assisted vegetables oil based minimum quantity lubrication for surface grinding of Ti–6AL–4V–ELI. *Tribology International*, 2020, 144: 106113
 140. Guo S M, Li C H, Zhang Y B, Wang Y G, Li B K, Yang M, Zhang X P, Liu G T. Experimental evaluation of the lubrication performance of mixtures of castor oil with other vegetable oils in MQL grinding of nickel-based alloy. *Journal of Cleaner Production*, 2017, 140: 1060–1076
 141. Wang X M, Li C H, Zhang Y B, Ali H M, Sharma S, Li R Z, Yang M, Said Z, Liu X. Tribology of enhanced turning using biolubricants: a comparative assessment. *Tribology International*, 2022, 107766
 142. Duan Z J, Li C H, Zhang Y B, Yang M, Gao T, Liu X, Li R Z, Said Z, Debnath S, Sharma S. Mechanical behavior and semiempirical force model of aerospace aluminum alloy milling using nano biological lubricant. *Frontiers of Mechanical Engineering*, 2023, 18(1): 4
 143. Xu W H, Li C H, Zhang Y B, Ali H M, Sharma S, Li R Z, Yang M, Gao T, Liu M Z, Wang X M, Said Z, Liu X, Zhou Z M. Electrostatic atomization minimum quantity lubrication machining: from mechanism to application. *International Journal of Extreme Manufacturing*, 2022, 4: 042003
 144. Jia D Z, Li C H, Zhang Y B, Yang M, Cao H J, Liu B, Zhou Z M. Grinding performance and surface morphology evaluation of titanium alloy using electric traction bio micro lubricant. *Journal of Mechanical Engineering*, 2022, 58(5): 198–211
 145. Yang Y Y, Gong Y D, Li C H, Wen X L, Sun J Y. Mechanical performance of 316L stainless steel by hybrid directed energy deposition and thermal milling process. *Journal of Materials Processing Technology*, 2021, 291: 117023
 146. Li H G, Zhang Y B, Li C H, Zhou Z M, Nie X L, Chen Y, Cao H J, Liu B, Zhang N Q, Said Z, Debnath S, Jamil M, Ali H M, Sharma S. Extreme pressure and antiwear additives for lubricant:

- academic insights and perspectives. *The International Journal of Advanced Manufacturing Technology*, 2022, 120(1–2): 1–27
147. Gao T, Li C H, Zhang Y B, Yang M, Jia D Z, Jin T, Hou Y L, Li R Z. Dispersing mechanism and tribological performance of vegetable oil-based CNT nanofluids with different surfactants. *Tribology International*, 2019, 131: 51–63